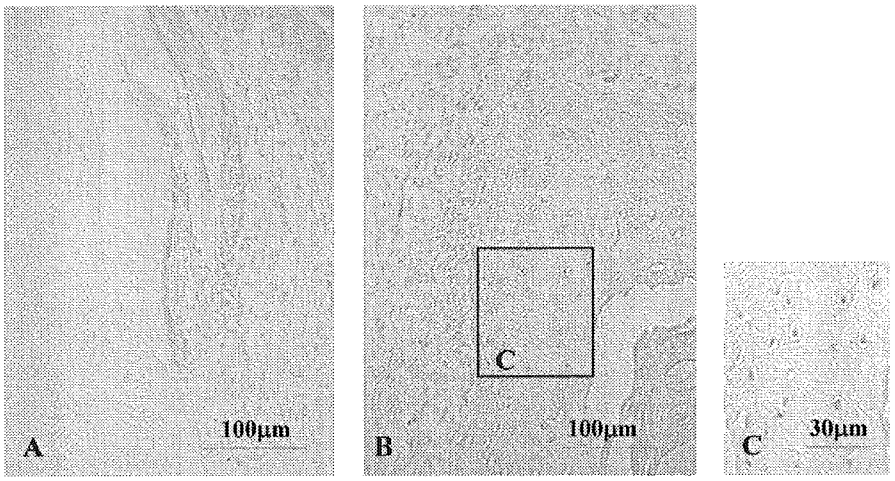

Figure 1 Immunohistochemical staining of COX-1 in the periodontal tissue of an untreated control rat. (A) Weakly positive staining is seen in the junctional epithelial cells facing the enamel surface. (B) Osteocytes embedded in alveolar bone stained weakly positive for COX-1. (C) Note positively stained osteocytes.

0.3% hydrogen peroxide in PBS to block the endogenous peroxidase activity for 1 h. The sections were rinsed with PBS, incubated with the peroxidase-conjugated streptavidin for 30 min and rinsed with PBS again. The color was developed with 0.025% 3-3′-diaminobenzidine tetrahydrochloride in Tris-HCl buffer plus hydrogen peroxide (Kyowa medics, Tokyo, Japan). The specimens were counter stained with Mayer's hematoxylin, dehydrated and then mounted.

Specificity was ascertained by substituting PBS and normal rabbit serum for each antibody.

Results

Untreated control periodontal tissue

In the normal gingival tissue of untreated control rats, small number of PMNs was seen in the junctional epithelium (JE) and sub-JE area but no obvious inflammatory changes were observed.

COX-1-positive cells were detected in the layer of JE, which faced the enamel surface (Fig. 1A). In the deep periodontal tissue, numerous osteocytes embedded in alveolar bone were weakly positive

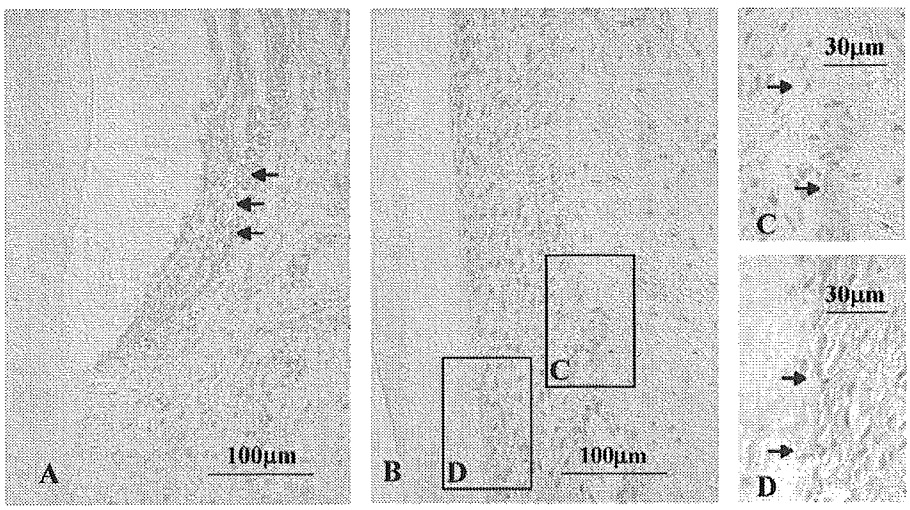

Figure 2 Immunohistochemical staining of COX-2 in the periodontal tissue of an untreated control rat. (A) Positive reaction is seen in the junctional epithelial cells located in the interfacing area to the oral sulcular epithelium (arrows) and macrophages in perivascular area. (B) Note osteoblasts and cementoblasts in the square area. (C) Arrows show positively stained osteoblasts lining the alveolar bone margin (periodontal ligament side). (D) Cementoblasts (arrows) are slightly positive for COX-2.

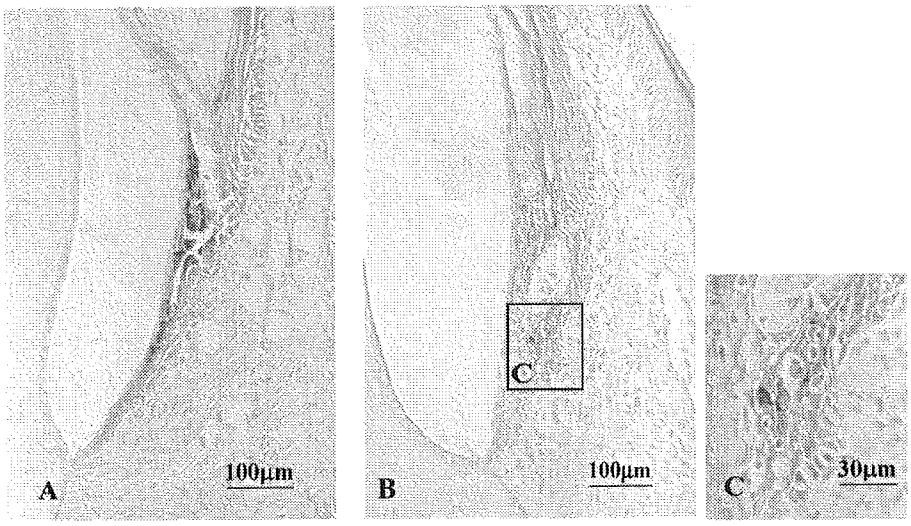

Figure 3 Immunohistochemical staining of COX-2 in the gingival tissue of LPS treated experimental rat. (A) At 1 h after topical application of LPS, almost all cells in the junctional epithelium are strongly positive for COX-2. (B, C) At 2 days after topical application of LPS, numerous COX-2 positive PMNs were seen in the enlarged spaces between COX-2 positive junctional epithelial cells and subjunctional epithelial area.

for COX-1 (Fig. 1B and C). Positive reaction for COX-1 could not be detect in other constitutive cells presented in periodontal tissue. A weakly positive reaction for COX-2 was seen not only in a small number of JE cells adjacent to the gingival sulcus but also in macrophages located in perivascular area (Fig. 2A). Osteoblasts lining the alveolar margin (Fig. 2B and C) and cementoblasts facing the cementum surface (Fig. 2B and D) were also weakly positive for COX-2.

LPS applied periodontal tissue

LPS application caused edematous changes, dilatation of blood capillaries and infiltration of PMNs in sub-JE area. Numerous PMNs migrated into enlarged intercellular spaces of the JE. These findings have appeared in 1-h specimens and continued until 3 days after LPS application. The inflammatory changes gradually decreased with time and disappeared by day 7.

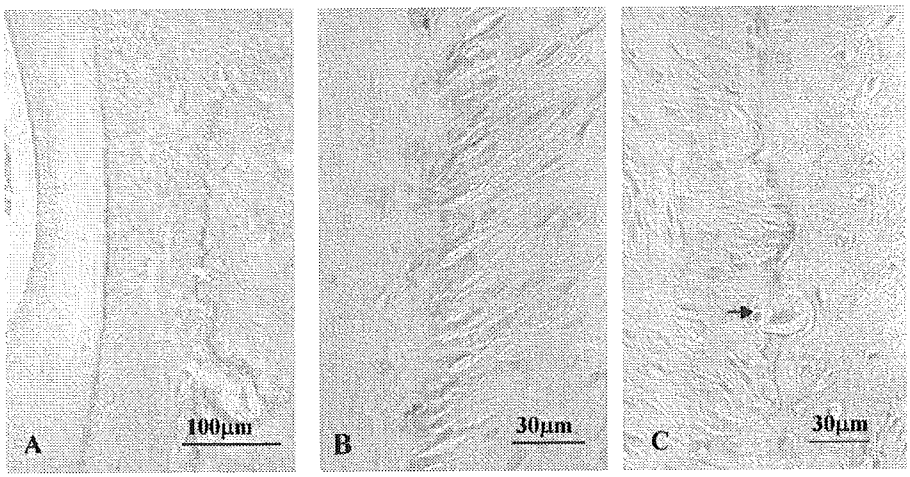

Figure 4 Immunohistochemical staining of COX-2 in the periodontal tissue of LPS treated experimental rat at 2 d after topical application of LPS. (A) Almost all cells facing the root surface and alveolar bone margin (periodontal ligament side) are strongly positive for COX-2. (B) Note the restriction of the cytoplasmic reaction to the tooth surface portion of cementoblasts. (C) The cytoplasmic reaction in osteoblasts is restricted to the alveolar bone side. An osteoclast (arrow) near the COX-2-positive osteoblasts is negatively stained.

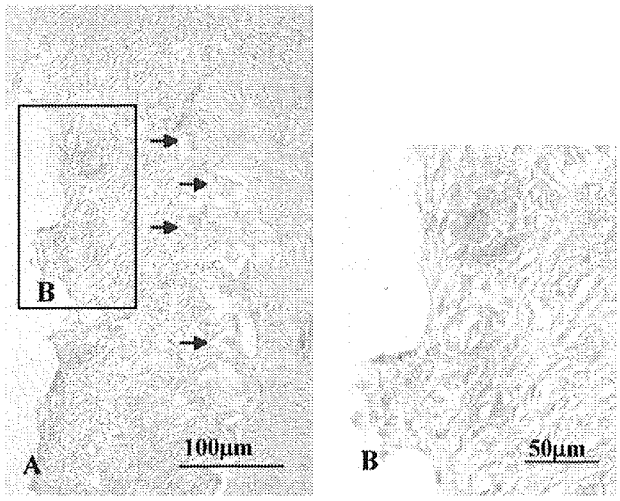

Figure 5 Immunohistochemical staining of COX-2 in the case with prominent periodontal tissue destruction of an LPS treated experimental rat at 3 d after topical application of LPS. (A) Strongly COX-2-expressed cells are seen in the alveolar crestal area of the periodontal ligament. Numerous osteoclasts (arrows) appearing along the alveolar bone margin were negative for COX-2. (B) The COX-2-expressed cells are round and spindle in shape.

LPS enhanced COX-2 expression in periodontal tissue at 3 h. In JE, numerous COX-2-positive cells were observed. Both of the number of COX-2-positive cells and the intensity of COX-2 expression reached a maximum at 1 day (Fig. 3A) and continued for 2 days (Fig. 3B). COX-2-positive epithelial cells were not detected in oral sulcular and oral gingival epithelium. Numerous PMNs with weak positivity for COX-2 were seen in the widely enlarged intercellular spaces among the COX-2 positive JE cells.

In deep periodontal tissue, an enhancement of COX-2 expression in osteoblasts and cementoblasts was detected (Fig. 4A). Almost all cells facing the root surface and alveolar bone surface, which seemed to be cementoblasts (Fig. 4B) and osteoblasts (Fig. 4C) respectively, were positively stained for COX-2 until 2 days after LPS application. Positive reaction in both of cementoblasts and osteoblasts was restricted to the cytoplasm facing to the tooth surface and the bone surface. In the case with severe periodontal tissue destruction at 3 days after, some COX-2-positive periodontal ligament cells, which were spindle or oval in shape, were seen near the resorbing bone and tooth surfaces (Fig. 5A and B). Osteoclasts increased in this period were negatively stained for COX-2 (Figs. 4C and 5A). The intensity of COX-2 expression and the number of COX-2 positive cells decreased and returned to the normal range by 7 days.

On the other hand, the density and distribution pattern of COX-1-positive cells in gingival and periodontal tissue remained unchanged during the experimental period.

Discussion

Since we employed a cotton roll applicator saturated with the LPS solution to avoid the periodontal tissue destruction caused by the application method, we needed a large amount of LPS to perform the present animal experiment. Therefore we used commercially available LPS from *E. coli* to provoke the initial periodontal tissue destruction in this study. *E. coli* is not a periodontal pathogen, but it is evident that LPS from *Actinobacillus actinomycetemcomitans*, which is one of principal periodontal pathogens, is similar to *E. coli*-LPS and shares numerous biological activities on the host cells with *E. coli*-LPS.[25]

We could successfully demonstrate the immunohistochemical localization of COX-1 and COX-2 in rat periodontal tissues. In the untreated control group, the weakly positive COX-1 reaction was observed in JE cells and osteocytes of alveolar bone. The density and distribution pattern of COX-1-positive cells in periodontal tissues remained unchanged during the experimental period. Several studies have reported that COX-1 is widely distributed and constitutively expressed in various cells, where PGs are needed for normal physiological function.[3] For example, the integrity of the stomach lining and normal renal function in the kidney are maintained by PGs synthesized by COX-1. It has been reported that the COX-1 protein expression in human OGE cells was not effected by stimuli of proinflammatory cytokine or serum.[26] In osteocyte-like MLO-Y4 cells, COX-1 mRNA is constitutively expressed and its level remained constant after mechanical strain.[27] The constitutive PGs production, which depends on COX-1, may play an important role on regulation of physiological functions in JE and alveolar bone.

In the untreated control group, not only COX-1 expression but also COX-2 expression was detected. COX-2 is weakly expressed in JE cells osteoblasts and cementoblasts. We previously observed that the coronal half of JE was positively stained for proinflammatory cytokines such as TNF-α, IL-1α and IL-1β in the normal gingival tissue.[24] It has been reported that keratinocytes can constitutively produce proinflammatory cytokines in vitro.[28] The cytokines have been demonstrated to be potent stimulator of PGE_2 production in a variety of cells.[29] These proinflammatory cyto-

kines may induce COX-2 expression in JE cells under normal conditions. There is another possibility that serum components may induce COX-2 expression in JE. Serum can cause PG production in several types of cells including fibroblasts, osteoblasts and epithelial cells.[30,31] Noguchi et al. reported that serum stimulated oral gingival epithelial cells produced significant levels of PGE_2 and that COX-2 protein and mRNA detected in serum stimulated oral gingival epithelial cells.[26] The JE cells may play a role in the first defense against continuously invading irritants from gingival sulcus by their PGs production via COX-2.

Interestingly osteoblasts and cementoblasts weakly expressed COX-2 under normal conditions. It is known that mechanical stress stimulates PGE_2 production in various cells such as fibroblasts, osteoblasts and periodontal ligament cells.[32–34] PGE_2 is considered one of the most important mediators transducing mechanical stimuli to biological stimuli. Shimizu et al. demonstrated that cyclic tension force induced COX-2 and the subsequent significant PGE_2 production from human periodontal ligament cells.[34] Periodontal ligament cells, especially cementoblasts on the tooth surface and osteoblasts on the alveolar bone surface are exposed to continuous cyclic tension force caused by occlusal pressure. The PGs production depending on COX-2 in osteoblasts and cementoblasts may be involved in remodeling of bone and cementum caused by occlusal pressure.

There are many studies have shown that COX-2 is the major inducible isoform responsible for PG production in periodontal disease site. Zhang et al.[20] demonstrated that the amounts of COX-2 mRNA and protein were elevated in gingival tissue from subjects with chronic periodontitis compared with those from healthy subjects. Cavenaugh et al. demonstrated that COX-2 protein is expressed in mononuclear inflammatory cells, endothelial cells, gingival fibroblasts and epithelial cells in inflamed human gingiva.[35] Morton and Dongari-Bagtzoglou also reported that COX-2 expression was detected in the gingival epithelium, endothelial cells, and gingival fibroblasts and that it was significantly higher in the tissues with high levels of inflammatory infiltrates.[19] In the present study, LPS application induced COX-2 production with a peak at 1 to 2 days in JE cells. Using this animal model, we revealed that inductive proinflammatory cytokine expression in JE cells at 3 h just before enhancement of COX-2 expression seen at 1–2 days after LPS application.[24] This suggests that COX-2 synthesis in JE cells directly stimulated by LPS or indirectly stimulated via pro-inflammatory cytokines production by LPS-stimulation may be responsible for the increased PGE_2 production and the excessive PGE_2 produced from JE cells may play an important role in the dilatation of blood vessels, edema and activation of inflammatory cells seen in the gingival connective tissue subjacent to JE.

At 2 days after LPS application, in addition to osteoblasts and cementoblasts, some periodontal ligament cells in the alveolar crestal area were positively stained for COX-2 in the periodontal tissue. The positive reaction in cementoblasts and osteoblasts was restricted to the cytoplasm facing the tooth surface and the bone surface, respectively. Moreover, numerous osteoclasts were present along the alveolar bone surface in this period. Our previous study using this animal model demonstrated that the number of osteoclasts showed a biphasic increase peaking at 3 h and 3 days after LPS application.[21] Furthermore pretreatment of indomethacin, an inhibitor of COX-1 and COX-2, reduced the second peak of osteoclast increase at 3 days after application of LPS (unpublished data). PGE_2 is well known to mediate osteoclastic bone resorption and connective tissue destruction via collagenase production.[13,36] In addition, it is reported that increase of PGE_2 level in gingival crevicular fluid is associated with attachment loss.[14–16] Therefore it is likely that LPS applied from gingival sulcus may induce a large amount of PGE_2 synthesis associated with COX-2 induction in bone surface and cementum surface area and may be involved in attachment loss and osteoclastic bone resorption, characteristic features of periodontitis.

NSAIDs such as indomethacin and flurbiprofen have been found effective in the prevention of periodontal destruction.[17] However, because NSAIDs inhibit not only the inducible PGs by COX-2 at periodontal disease site but also the cytoprotective PGs by COX-1, the long term administration of NSAIDs for controlling periodontitis can cause side effects such as gastric ulcer, bleeding and renal dysfunction.[37] Recently it has been reported that selective inhibition of COX-2 inhibitors may be useful for the prevention and treatment of chronic arthritis[5] and periodontal disease[18] with the advantage of reduced toxicity.

In conclusion, (1) some JE cells constitutively expressed both COX-1 and COX-2 proteins. There is a possibility that the constitutive expression of COX-2 in JE cells may associate with continuously invading irritant such as normal oral microflora from gingival sulcus. (2) After LPS application, JE cells rapidly reacted with LPS stimulation and increased expression of COX-2. This finding suggests that JE cells may play a critical role in the first line of defense against LPS challenge and that PGE_2 pro-

duced by JE cells via COX-2 may be responsible for the initiation of inflammation. (3) LPS application caused a transient up-regulation of COX-2 expression in cementoblasts, periodontal ligament cells and osteoblasts. This suggests that PGE_2 from these cells in periodontal tissue may be associated with connective tissue destruction and bone resorption.

Further studies will be required to clarify the critical role of PGE_2 production via COX-2 in the pathogenesis of periodontitis and the possibility of establishment of new periodontal therapy using selective COX-2 inhibitors.

References

1. Garrison SW, Nichols FC. LPS-elicited secretory responses in monocytes: Altered release of PGE_2 IL-1β in patients with adult periodontitis. *J Periodont Res* 1989;**24**:88–95.
2. Lindemann RA, Economou JS, Rothermel H. Production of interleukin-1 and tumor necrosis factor by human peripheral monocytes activated by periodontal bacteria and extracted lipopolysaccharides. *J Dent Res* 1988;**67**:1131–5.
3. O'Neil GP, Ford-Hutchinson AW. Expression of mRNA for cyclooxygenase-1 and cyclooxygenase-2 in human tissue. *FEBS Lett* 1993;**330**:156–60.
4. Howell GL. Cytokine networks in destructive periodontal disease. *Oral Dis* 1996;**1**:266–70.
5. Katori M, Majima M, Harada Y. Possible background mechanisms of the effectiveness of cyclooxygenase-2 inhibitors in the treatment of rheumatoid arthritis. *Inflamm Res* 1998;**47**:S107–11.
6. Okada H, Murakami S. Cytokine expression in periodontal health and disease. *Crit Rev Oral Biol Med* 1998;**9**:248–66.
7. Smith WL, Song I. The enzymology of prostaglandin endoperoxide H syntheses-1 and -2. *Prostaglandins Other Lipid Mediat* 2002;**68/69**:115–28.
8. Jones DA, Carlton DP, Mclntyre TM, Zimmerman GA, Prescott SM. Molecular cloning of human prostaglandin endoperoxide synthase type II and demonstration of expression in response to cytokines. *J Biol Chem* 1993; **268**:9049–54.
9. Lee SH, Soyoola E, Chanmugam P, et al. Selective expression of mitogen-inducible cyclooxygenase in macrophages stimulated with lipopolysaccharide. *J Biol Chem* 1992;**267**: 25934–8.
10. Kraemer SA, Meada EA, DeWitt DL. Prostaglandin endoperoxide synthase gene structure: identification of the transcriptional start site and 5′-flanking regulatory sequence. *Arch Biochem Biophys* 1992;**293**:391–400.
11. Kujibu DA, Hershman HR. Dexamethason inhibits mitogen induction of the TIS10 prostaglandin synthase/cyclooxygenase gene. *J Biol Chem* 1992;**267**:7991–4.
12. Miyauchi M, Ijuhin N, Nikai H, Takata T, Ito H, Ogawa I. Effect of exogenously applied prostaglandin E2 on alveolar bone loss—Histometric analysis. *J Periodontol* 1992;**63**: 405–11.
13. Sterret JD. The osteoclast and periodontitis. *J Clin Periodontol* 1986;**13**:258–64.
14. Offenbacher S, Odle BM, Van Dyke TE. The use of crevicular fluid prostaglandin E2 levels as a predictor of periodontal attachment loss. *J Periodont Res* 1986;**21**:101–12.
15. Offenbacher S, Heasman PA, Collins GJ. Modulation of host PGE_2 secretion as a determinant of periodontal disease expression. *J Periodontol* 1993;**64**:432–44.
16. Preshaw PM, Heasman PA. Prostaglandin E2 concentrations in gingival crevicular fluid: observations in untreated chronic periodontitis. *J Clin Peiodontol* 2002;**29**:15–20.
17. Howell TH, Williams RC. Nonsteroidal anti-inflammatory drugs as inhibitors of periodontal disease progression. *Critical Rev Oral Biol Med* 1993;4:177–96.
18. Lohinai Z, Stachlewits R, Szekely AD, Feher E, Dezsi L, Szabo C. Evidence for the expression of cyclooxygenase-2 enzyme in periodontitis. *Life Sci* 2001;**70**:279–90.
19. Morton RS, Dongari-Bagtzoglou AI. Cyclooxygenase-2 is upregulated in inflamed gingival tissues. *J Periodontol* 2001;**72**:461–9.
20. Zahng F, Engebretson SP, Morton RS, Cavanaugh PF, Subbaranaiah K, Dannenberg AJ. The overexpression of cyclo-oxygenase-2 in chronic periodontitis. *JADA* 2003; **134**:61–7.
21. Ijuhin N. Light and electron microscopic studies of experimentally-induced pathologic changes in the rat periodontal tissue. *Adv Dent Res* 1998;**2**:209–14.
22. Miyauchi M, Takata T, Ito H, Ogawa I, Kudo Y, Takekoshi T, et al. Distribution of macrophage lineage cells in rat gingival tissue after topical application of lipopolysaccharide: an Immunohistochemical study using monoclonal antibodies: OX6, ED1 and ED2. *J Periodont Res* 1998;**33**:345–51.
23. Ijuhin N, Miyauchi M, Ito H, Takata T, Ogawa I, Nikai H. Enhanced collagen phagocytosis by rat molar periodontal fibroblasts after topical application of lipopolysaccharide—ultrastructural observations and morphometric analysis. *J Periodont Res* 1992;**27**:167–75.
24. Miyauchi M, Sato S, Kitagawa S, Hiraoka M, Kudo Y, Odawa I, et al. Cytokine expression in rat molar gingival periodontal tissues after topical application of lipopolysaccharide. *Histochem Cell Biol* 2001;**116**:57–62.
25. Schytte Blix IJ, Helgeland K, Hvattum E, Lyberg T. Lipopolysaccharide from *Actinobacillus actinomycetemcomitans* stimulates production of interleukin-1beta, tumor necrosis factor-alpha. *J Periodontal Res* 1999;**34**:4–40.
26. Noguchi K, Shitashige M, Endo H, Kondo H, Yotsumoto Y, Izumi Y, et al. Involvement of cyclooxygenase-2 in serum-induced prostaglandin production by human oral gingival epithelial cells. *J Periodont Res* 2001;**36**:124–30.
27. Cheng B, Kato Y, Zhao S, Luo J, Sprague E, Bonewald LF, et al. PGE_2 is essential for gap junction-mediated intercellular communication between osteocyte-like MLO-Y4 cells in response to mechanical strain. *Endocrinology* 2001;**142**:3464–73.
28. Hillmann G, Hillmann B, Geurtsen W. Immunohistochemical determination of interleukin-β in inflamed human gingival epithelium. *Archs Oral Biol* 1995;**40**:353–9.
29. Yuchel-Lindberg T, Nilsson S, Modeer T. Signal transduction pathways involved in the synergistic stimulation of prostaglandin production by interleukin-β and tumor necrosis factor α in human gingival fibroblasts. *J Dent Res* 1999;**78**:61–8.
30. Wadleigh DJ, Herschman HR. Transcriptional regulation of the cyclooxygenase-2 gene by diverse ligands in murine osteoblasts. *Biochem Biophys Res Commun* 1999;**264**: 865–70.
31. Xie W, Herschman HR. Transcriptional regulation of prostaglandin synthase 2 gene expression by platelet-derived growth factor and serum. *J Biol Chem* 1996;**271**:31742–8.
32. Almekinders LC, Banes AJ, Ballenger CA. Effects of repetitive motion on human fibroblasts. *Med Sci Sports Exerc* 1993;**25**:603–7.

33. Bakker AD, Klein-Nulend J, Burger EH. Mechanotransduction in bone cells proceeds via activation of COX-2, but not COX-1. *Biochem Biophys Res Commun* 2003;**305**: 677–83.
34. Shimizu N, Ozawa Y, Yamaguchi M, Goseki T, Ohzeki K, Abiko Y. Induction of COX-2 expression by mechanical tension force in human periodontal ligament cells. *J Periodontol* 1998;**69**:670–7.
35. Cavanaugh Jr PF, Mcdonald JS, Pavelie L, Limardi RJ, Glickman JL, Pavelic ZP. Immunohistochemical localization of prostaglandin H synthase isozyme proteins in the gingival tissue of patients with periodontitis. *Inflammopharmacology* 1995;**3**:109–19.
36. Wahl LM, Mergenhagen SE. Regulation of monocyte/macrophage collagenase. *J Oral Pathol* 1998;**17**:452–5.
37. Vane JR. Towerds a better aspirin. *Nature* 1994;**367**:215–6.

INFECTION AND IMMUNITY, Feb. 2004, p. 871–879 Vol. 72, No. 2
0019-9567/04/$08.00+0 DOI: 10.1128/IAI.72.2.871–879.2004

Caspase-2 and Caspase-7 Are Involved in Cytolethal Distending Toxin-Induced Apoptosis in Jurkat and MOLT-4 T-Cell Lines

Masaru Ohara,[1] Tomonori Hayashi,[2] Yoichiro Kusunoki,[2] Mutsumi Miyauchi,[3] Takashi Takata,[3] and Motoyuki Sugai[1]*

Departments of Bacteriology[1] and Oral Maxillofacial Pathology,[3] Hiroshima University Graduate School of Biomedical Sciences, Hiroshima 734-8553, and Department of Radiobiology and Molecular Epidemiology, Radiation Effects Research Foundation, Hiroshima 732-0815,[2] Japan

Received 20 May 2003/Returned for modification 12 August 2003/Accepted 22 October 2003

Cytolethal distending toxin (CDT) from *Actinobacillus actinomycetemcomitans* is a G_2/M cell-cycle-specific growth-inhibitory toxin that leads to target cell distension followed by cell death. To determine the mechanisms by which *A. actinomycetemcomitans* CDT acts as an immunosuppressive factor, we examined the effects of highly purified CDT holotoxin on human T lymphocytes. Purified CDT was cytolethal toward normal peripheral T lymphocytes that were activated by in vitro stimulation with phytohemagglutinin. In addition, purified CDT showed cytolethal activity against Jurkat and MOLT-4 cells, which are known to be sensitive and resistant, respectively, to Fas-mediated apoptosis. Death in these cell lines was accompanied by the biochemical features of apoptosis, including membrane conformational changes, intranucleosomal DNA cleavage, and an increase in caspase activity in the cells. Pretreatment of Jurkat cells with the general caspase inhibitor z-VAD-fmk mostly suppressed CDT-induced apoptosis. Furthermore, specific inhibitors of caspase-2 and -7 showed significant inhibitory effects on CDT-induced apoptosis in Jurkat cells, and these inhibitory effects were fully associated with reduced activity of caspase-2 or -7 in the CDT-treated Jurkat cells. These results strongly suggest that CDT possesses the ability to induce human T-cell apoptosis through activation of caspase-2 and -7.

Bacterial infections in mammals evoke a series of immune reactions to bacterial antigens in the infected host, but immune responses are occasionally suppressed or shut down by some bacterial products, such as toxins. Suppression or inactivation of the host immune response is considered to be a bacterial strategy to evade host immune mechanisms. *Actinobacillus actinomycetemcomitans* is a gram-negative rod-shaped pathogen implicated in the pathogenesis of juvenile and adult periodontitis (38). Previous studies demonstrated that *A. actinomycetemcomitans* produces a factor(s) that is immunosuppressive for human T and B cells (25). It was recently established that *A. actinomycetemcomitans* produces a new member of the cytolethal distending toxin (CDT) family which was previously unrecognized as a virulence factor of *A. actinomycetemcomitans* (40). CDT belongs to the family of toxins with cell-cycle-specific inhibitory activities which block the progression of cells from G_2 to M phase (28). CDT-poisoned cells undergo cell distension and nucleus swelling and eventually die. CDT was found to form a complex of three subunits, CDTA, -B, and -C (9, 14, 21, 24, 31, 40), and the subunits were determined to be tandemly encoded by the *cdtA*, *cdtB*, and *cdtC* genes at the chromosomal *cdt* loci. *A. actinomycetemcomitans* CDTA, -B, and -C are translated as approximately 25-, 32-, and 21-kDa proteins, respectively, and are secreted into the periplasm (40). After cleavage of their 15- to 21-amino-acid signal sequences at the N terminus, they become 23-, 29-, and 19-kDa proteins, respectively (31, 36, 40). CDTA goes through another processing step to become an 18- to 19-kDa form, designated CDTA′, and forms a complex with CDTB and CDTC to become a holotoxin (40).

In 1999, Shenker et al. purified the immunosuppressive factor of *A. actinomycetemcomitans* that could affect human T cells and demonstrated that the factor was one of the subunit proteins of CDT, CDTB (34, 36). Their group also demonstrated that a crude CDT preparation of *A. actinomycetemcomitans* induced cell cycle arrest at the G_2 phase in human peripheral blood cells (37). Furthermore, the CDT preparation was shown to induce apoptotic cell death in peripheral blood lymphocytes along with activation of caspase-3, -8, and -9 (35). Despite those findings, whether these caspases are really involved in CDT-induced apoptosis remains virtually unknown.

For this study, we studied the immunosuppressive effect of highly purified *A. actinomycetemcomitans* CDT on normal human T lymphocytes and made an in-depth characterization of the cytolethal effect by using the T-cell leukemia cell lines Jurkat and MOLT-4, which are sensitive and resistant, respectively, to Fas-mediated apoptosis. We herein demonstrate that CDT induces apoptosis in these cells and that caspase-2 and -7 play important roles in the signaling pathway of CDT-induced cell death, which is distinct from Fas-mediated apoptosis.

MATERIALS AND METHODS

Purification of *A. actinomycetemcomitans* CDT. CDT holotoxin was prepared by using the pQE 60 (C-terminal histidine tag) protein expression system in M15 *Escherichia coli* (Qiagen, Tokyo, Japan). Briefly, for construction of pQE*cdtABC*, the *A. actinomycetemcomitans cdtABC* gene was isolated from *A. actinomycetemcomitans* genomic DNA by PCR amplification with specific primers that contained several restriction enzyme sites for subcloning into vectors, as follows: QIA-U, 5′-AGGTA*CCATGG*AAAAGTTT-3′, which corresponds to the *cdtA* starting site with an *Nco*I restriction enzyme site; QIC-L, 5′-AA*GATCT*GCT ACCCTGA-3′, which corresponds to the end of the *cdtC* gene, with the stop

* Corresponding author. Mailing address: Department of Bacteriology, Hiroshima University Graduate School of Biomedical Sciences, Kasumi 1-2-3, Minami-ku, Hiroshima, Hiroshima 734-8553, Japan. Phone: (81) 82 257 5635. Fax: (81) 82 257 5639. E-mail: sugai@hiroshima-u.ac.jp.

codon replaced with a *Bgl*II site (restriction sites are shown in italics). The amplified *cdtABC* gene was ligated into pQE60 in frame at the *Nco*I and *Bgl*II sites, so that the C-terminal CDTC was tagged with six histidine residues. The expression of the *cdtABC* gene was induced by adding isopropyl-β-D-1-thiogalactopyranoside (final concentration of 1 mM; Sigma) at an optical density at 660 nm of 0.5 to 0.7. After induction for 4 h, the culture supernatant was harvested by centrifugation at 5,000 × *g* for 5 min, and crude proteins were precipitated with ammonium sulfate (final concentration, 80%) by gentle stirring for at least 4 h. The precipitates were recovered by centrifugation at 15,000 × *g* for 20 min, dissolved in phosphate-buffered saline (PBS) (137 mM NaCl, 2.7 mM KCl, 8.1 mM Na_2HPO_4, 1.5 mM KH_2PO_4), and dialyzed overnight against PBS. Ni-chelated agarose beads were added into the dialyzed solution and gently shaken for at least 1 h, followed by column chromatography. The column was washed with washing buffer (50 mM NaH_2PO_4 [pH 8.0], 300 mM NaCl, 20 mM imidazole) and eluted with elution buffer (50 mM NaH_2PO_4 [pH 8.0], 300 mM NaCl, 250 mM imidazole). The eluted CDT holotoxin was dialyzed against PBS and concentrated with Centricon 10 concentrators (Millipore, Bedford, Mass.).

Preparation of cells and culture conditions. Peripheral blood mononuclear cells were obtained from healthy volunteers with their informed consent. Twenty to forty milliliters of heparinized venous blood was diluted with an equal volume of PBS with 1% heparin and layered over Ficoll-Hypaque lymphocyte separation medium (ICN Biomedical Inc., Aurora, Ohio). Density gradient centrifugation was performed at 400 × *g* for 30 min, and mononuclear cells were harvested from the plasma-lymphocyte separation medium interface. Collected cells were washed twice with Earle's balanced salt solution (Nissui, Tokyo, Japan) containing 2.5% fetal calf serum (FCS) (Intergen Co., Purchase, N.Y.). The number of recovered cells was counted and diluted to 10^6 cells/ml in RPMI 1640 containing 10% FCS, 100 U of penicillin G/ml, and 100 μg of streptomycin/ml. The isolated lymphocytes were incubated with CDT (100 ng/ml) and cultured at 37°C in 5% CO_2, with or without stimulation on day 1 by phytohemagglutinin (PHA) (Difco Lab., Detroit, MI) diluted 1:1,600, and the cell population was monitored for 96 h. A thymic T-cell leukemia cell line, MOLT-4, and a peripheral T-cell leukemia cell line, Jurkat, were maintained in RPMI 1640 containing 10% FCS and 25 μg of kanamycin/ml at 37°C in 5% CO_2. The cells (10^6 cells/ml) were left untreated or were treated with CDT (100 ng/ml) and cultured under similar conditions. In some experiments, Jurkat cells were similarly treated with 100 ng of anti-CD95 (anti-Fas) monoclonal antibody (Ab) CH11 (BD PharMingen, San Diego, Calif.) per ml.

Flow cytometry. Conformational changes of the membrane by phosphatidylserine translocation and membrane hole formation were observed by counting the percentages of cells that were stained with fluorescein isothiocyanate (FITC)-labeled annexin V and propidium iodide (PI) in a FACScan flow cytometer (BD Biosciences, San Jose, Calif.). Briefly, CDT-treated cells (5×10^5 to 10×10^5) were collected by centrifugation at 350 × *g* for 2 min and were washed three times with 500 μl of PBS with 1% FCS. The washed cells were resuspended in 180 μl of PBS with 1% FCS, and 0.5 μl of FITC-labeled annexin V and 1 μl of PI, from the MEBCYTO apoptosis kit (MBL, Nagoya, Japan) were added to the cell suspension. After the reaction for 5 min at room temperature, 10,000 cells were analyzed in the FACScan instrument. The data obtained were processed by quadrant population analysis, using CellQuest software (BD Biosciences). The living cell population was determined by counting cells that were negative for both annexin V and PI (distributed in the lower left of the quadrant).

Caspase assay. CDT-treated cells were harvested and washed with PBS. PBS-washed cells were lysed with lysis buffer (10 mM Tris-Cl [pH 7.4], 25 mM NaCl, 0.25% Triton X-100, 1 mM EDTA) and centrifuged at 15,000 × *g* for 10 min. The supernatant was diluted with the lysis buffer and the protein concentration was adjusted to 1 mg/ml. Ten micrograms of total protein was incubated in 200 μl of caspase buffer (50 mM Tris-Cl [pH 7.2], 100 mM NaCl, 1 mM EDTA, 10% sucrose, 0.1% CHAPS, and 5 mM dithiothreitol) with a 50 μM concentration (each) of various fluorogenic substrate peptides. The peptides include Ac-DEVD-7-amino-4-methyl cumarine (AMC) for caspase-3, -7, and -8, Ac-DQTD-AMC for caspase-7 and -3, Ac-IETD-AMC for caspase-8, -6, and granzyme, Ac-LEHD-AMC for caspase-9, and Ac-VDVAD-AMC for caspase-2 (Peptide Institute Inc., Osaka, Japan).

The reaction mixture was incubated at 37°C for 60 min, and the release of 7-amino-4-methylcumarin was measured by use of a spectrophotometer (Shimazu RF-540), with excitation at 380 nm and emission at 460 nm. One unit (U) was defined as 5.2 pmol of substrate cleaved per min per mg of protein.

Various caspase inhibitors were used at a concentration of 100 μM. They were Ac-VAD-fmk as a general caspase inhibitor, Ac-WEHD-CHO for caspase-1, Ac-DEVD-CHO for caspase-3, -7, and -8, Ac-DMQD-CHO for caspase-3, Ac-LEHD-CHO for caspase-9, Ac-IETD-CHO for caspase-8 and -6, Ac-DQTD-CHO for caspase-7 and -3, and Ac-VDVAD-CHO for caspase-2 (Peptide Institute Inc.).

Electron microscopy. Cells were fixed with 2.5% glutaraldehyde for 2 h and rinsed in 0.1 M cacodylate buffer (pH 7.4) for 12 h. After postfixation with 1% osmium tetroxide for 30 min, cells were stained with 2% uranyl acetate for 30 min and dehydrated in graded alcohol, which was then replaced by propylene oxide. After these steps, the cell suspension was spun down at 8,000 × *g* for 5 min and the supernatant was discarded. The cell pellets were embedded in epoxy resin. Thin sections were stained in 2% uranyl acetate and lead citrate and were observed in a Hitachi H500 electron microscope.

Preparation of cytosolic and mitochondrial fractions. CDT-treated cells were washed twice with PBS and resuspended in isotonic buffer (10 mM HEPES [pH 7.3], 0.3 M mannitol, 0.1% bovine serum albumin). Digitonin was added to the cell suspension at a concentration of 0.1 mM, and the cells were incubated for 5 min on ice. After the samples were centrifuged at 8,500 × *g* for 5 min at 4°C, the supernatant was used as the cytosolic fraction. The pellet was resuspended in sonication buffer (50 mM Tris-HCl [pH 7.4], 150 mM NaCl, 2 mM EDTA, 1 mM phenylmethylsulfonyl fluoride, 0.5% Tween 20). The samples were sonicated with an ultrasonic disrupter (UD200 TOMY) for 20 s at output level 4. After centrifugation at 10,000 × *g* for 5 min at 4°C, the supernatant was collected and used as the mitochondrial fractions.

Antibodies. Antibodies against CDTA, -B, and -C that were previously obtained were used under conditions that were described elsewhere (40). Anti-cytochrome *c* Ab (BD PharMingen) was used according to the instructions provided by the supplier.

RESULTS

Cytolethal effects of highly purified CDT on human peripheral lymphocytes. *A. actinomycetemcomitans* CDT was purified from the culture supernatant of *E. coli* carrying the *A. actinomycetemcomitans cdtABC* genes. The secreted CDT complex was purified through a Ni chelation column, using the affinity of six histidine (His) residues tagged to the C terminus of CDTC (Fig. 1A). Sodium dodecyl sulfate-polyacrylamide gel electrophoresis and immunoblotting detected CDTA′, CDTB, and CDTC tagged with six histidine residues in the medium fraction, and premature CDTA was also found in a small amount, suggesting that most of the CDT complex consisted of CDTA′, CDTB, and CDTC. Cell distension and the G_2/M blocking activity of purified CDT were confirmed in HeLa cells, and the purified CDT complex was used for experiments.

To address whether CDT can induce cell death of human peripheral lymphocytes, we added purified CDT to peripheral blood mononuclear cell cultures in the presence or absence of PHA stimulation. Flow cytometry analysis with FITC-annexin V and PI revealed that treatment of normal lymphocytes with a combination of CDT and PHA increased the percentage of dead cells (the sum of annexin V^+ PI^+ and annexin V^+ PI^- fractions) (Fig. 1B). It should be noted that CDT did not kill lymphocytes very much unless they were activated with PHA. This is in good agreement with the previously suggested activity of CDT, which is cell-cycle-dependent cytotoxicity against HeLa cells (1), and also suggests that CDT can act as an immunosuppressive toxin by killing activated lymphocytes.

CDT induced apoptosis in Jurkat and MOLT-4 cells. In order to obtain further insights into the cytolethal effect of CDT in T lymphocytes, we used two cell lines, Jurkat and MOLT-4, and monitored population changes in four panels (upper left, upper right, lower left, and lower right [UL, UR, LL, and LR, respectively]) after CDT treatment (Fig. 2). For both cell lines, CDT treatment increased the percentage of dead cells (Fig. 2A). Flow cytometry analysis revealed that the percentage of annexin V^+ PI^- Jurkat cells (distributed in the

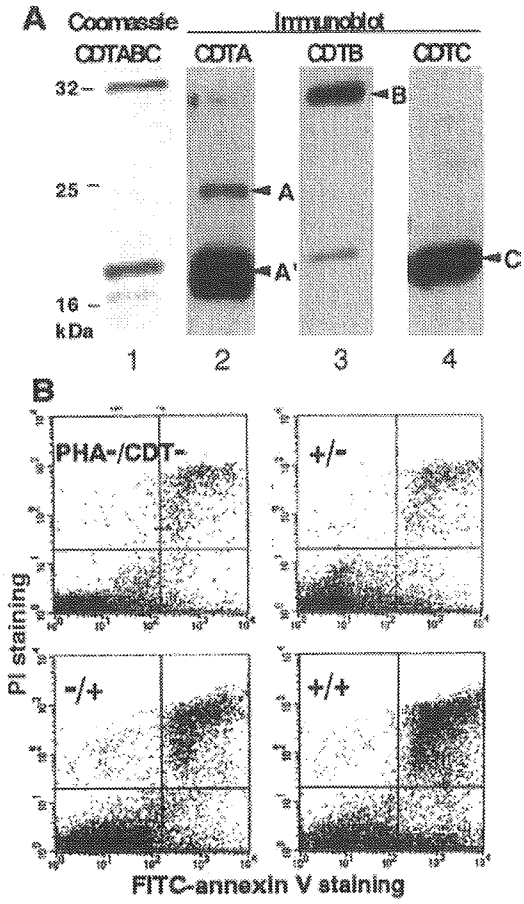

FIG. 1. Cytolethal effect of *A. actinomycetemcomitans* CDT on human peripheral lymphocytes. (A) Purified CDTABC complex in the medium fraction from *E. coli* M15 carrying *A. actinomycetemcomitans cdtABC*. Lane 1, Coomassie staining of CDTABC complex; lanes 2 to 4, immunoblots for the detection of each subunit by use of antiserum against CDTA, CDTB, and CDTC, respectively. Arrowheads: A, CDTA (premature form); A′, CDTA′ (mature form of CDTA); B, mature CDTB; C, mature CDTC tagged with six histidine residues. (B) Flow cytometry analysis. Lymphocytes were stained with FITC-labeled annexin V and PI and analyzed in a FACScan flow cytometer. Lymphocytes prepared from peripheral blood obtained from healthy human volunteers were treated with several combinations of PHA (1:1,600) and CDT (100 ng/ml). A representative result of the quadrant analysis of annexin V- and PI-stained lymphocytes on day 2 is shown.

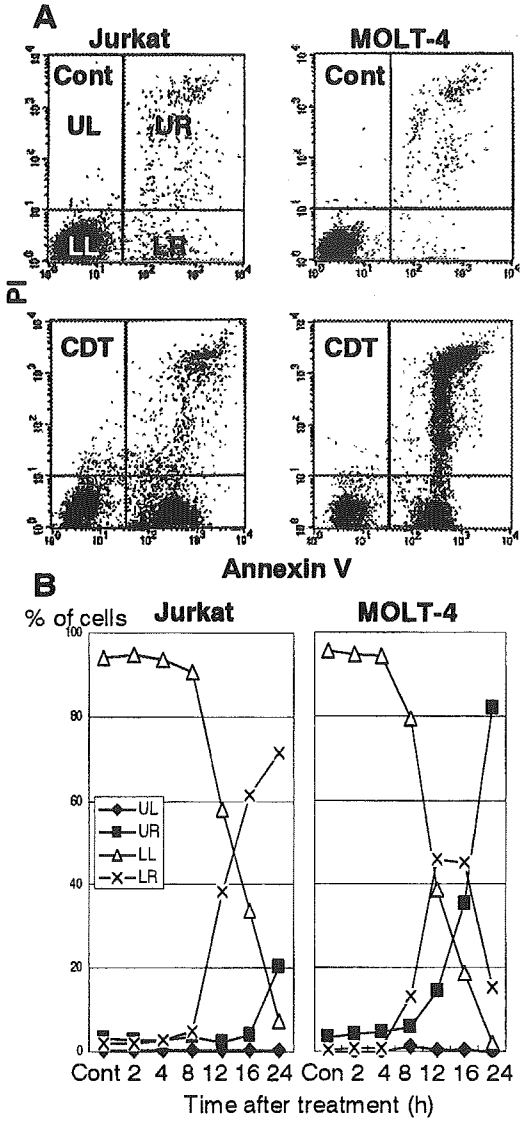

FIG. 2. Cytolethal kinetics on CDT-treated cell lines. T-cell leukemia cell lines Jurkat and MOLT-4 were treated with CDT (100 ng/ml) for various times. Cells stained with FITC-labeled annexin V and PI were analyzed by flow cytometry. (A) Representative results for cells with or without treatment of CDT at 16 h. Cont, control. (B) Kinetics of cell death measured at indicated times after CDT treatment. The percentages of cell populations in the UL quadrant (annexin V^- PI^+, ◆), the UR quadrant (annexin V^+ PI^+, ■), the LL quadrant (annexin V^- PI^-, △), and the LR quadrant (annexin V^+ PI^-, ×) are indicated.

LR panel) started to increase 8 h after CDT treatment and continued to increase until 24 h after treatment (Fig. 2B). MOLT-4 showed a somewhat different pattern from that of Jurkat. The percentage of annexin V^+ PI^- MOLT-4 cells (LR) started to increase 4 h after CDT treatment and reached a plateau 12 to 16 h after the treatment (Fig. 2B). After that, the annexin V^+ PI^- population (LR) decreased after 16 h. Concomitantly with the increase and decrease of the annexin V^+ PI^- population (LR), the annexin V^+ PI^+ population (UR) started to increase after 8 h and kept increasing until 24 h. In both cell lines, the increase of the annexin V^+ PI^- cell population (LR) in the early stage after treatment strongly suggested that CDT poisoning was able to induce apoptosis in cells that are sensitive to Fas-mediated apoptosis as well as in those that are resistant to Fas-mediated apoptosis. We further investigated the apoptotic characteristics of CDT-poisoned cells, including chromosomal DNA fragmentation and chromatin condensation. As shown in Fig. 3A, electrophoretic analysis of the chromosomal DNA of Jurkat cells showed a typical DNA ladder formation after 16 h of treatment with CDT, which is similar to those observed after treatment with anti-Fas Ab or irradiation. Electron microscopic observation of CDT-poisoned Jurkat cells revealed chromatin condensation, which is associated with cells undergoing apoptosis (Fig. 3B). Similar apoptotic characteristics were also apparent for CDT-treated MOLT-4 cells (data not shown). There was no necrotic change,

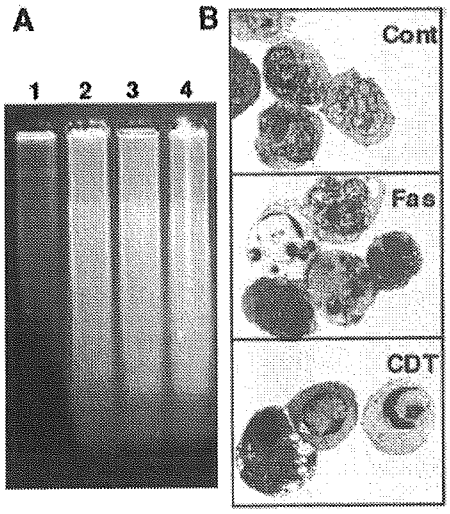

FIG. 3. Apoptotic DNA fragmentation and morphological change in CDT-treated lymphocytes. (A) DNA ladder formation in CDT-treated cells. Jurkat cells were treated with anti-Fas Ab (100 ng/ml) (lane 2), X-ray irradiation (10 Gy) (lane 3), or CDT (100 ng/ml) (lane 4) for 16 h, and chromosomal DNAs were prepared. The extracted DNAs were separated by agarose gel electrophoresis and visualized by staining with ethidium bromide. Lane 1, DNA from untreated Jurkat cells. (B) Ultrastructure of CDT- or anti-Fas Ab-treated lymphocytes. Jurkat cells were treated with CDT (100 ng/ml) for 16 h and subjected to electron microscopic observation as described in Materials and Methods. Cont, control.

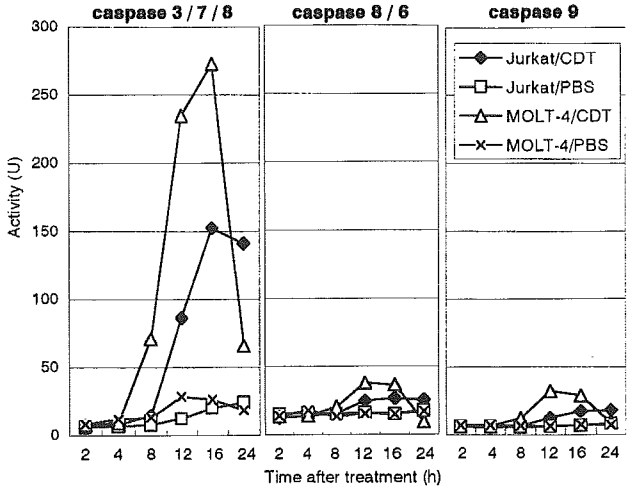

FIG. 4. Caspase activity in CDT-treated lymphocytes. The total protein (10 μg) was extracted from CDT-treated Jurkat or MOLT-4 cells at the indicated times. Caspase activity was measured by incubation of the extract with a fluorogenic substrate for caspase-3, -7, and -8 (left), caspase-8 and -6 (middle), or caspase-9 (right). After incubation, the released 7-amino-4-methylcumarine was measured in spectrophotometer, with excitation at 380 nm and emission at 460 nm. ◆, CDT-treated Jurkat cells; □, PBS-treated Jurkat cells (control); △, CDT-treated MOLT-4; ×, PBS-treated MOLT-4 (control). The experiments were repeated at least three times, and similar results were obtained. Representative results are shown.

such as swelling of the cell body and mitochondria or collapse of the plasma and nuclear membranes, in these cell lines.

Intracellular caspase activities. Apoptosis generally involves the activation of cysteine proteases, or caspases. The activity of sets of the major caspases, caspase-3, -7, and -8, caspase-8 and -6, and caspase-9, in Jurkat and MOLT-4 cells was monitored after CDT treatment. In Jurkat cells, the activity of caspase-3, -7, and -8 started to increase 8 h after treatment of the cells with CDT and significantly increased until 16 to 24 h (Fig. 4). On the other hand, the activity of the caspase-8 and -6 set and caspase-9 slightly increased upon treatment with CDT. Interestingly, caspase activity in MOLT-4 cells started to increase earlier and occurred at a higher level than in Jurkat cells between 4 and 16 h after treatment. After 12 to 16 h, caspase activity in MOLT-4 cells went down in parallel with the appearance of the annexin V^+ PI^- cell population (Fig. 4, Fig. 2B).

Cells retained the phenotype of living cells (annexinV^- PI^-) when the cells were pretreated with a general caspase inhibitor, z-VAD-fmk (100 μM), indicating that z-VAD-fmk is able to nearly completely inhibit CDT-induced apoptosis (Fig. 5A and B). It also turned out that the CDT-induced elevation of caspase activity could be blocked by z-VAD-fmk (Fig. 5C). These results indicated that CDT-induced apoptotic cell death in Jurkat and MOLT-4 cells was mostly dependent on the activation of a caspase(s) until at least 24 h after treatment.

Signaling pathway of caspases. Caspases can be classified into two categories as follows: initiator caspases, including caspase-2, -8, and -9, which are present upstream of the signaling pathway of apoptosis, and effector caspases, which play roles in the cleavage of many regulatory proteins (3). In order to determine the signaling pathway of the caspase(s) in CDT-induced apoptosis, we added a variety of caspase inhibitors and monitored their inhibitory effects on CDT cytotoxicity and apoptotic features in Jurkat cells by using flow cytometry with annexin V-PI double staining. For Fas-mediated apoptosis, caspase-8 was confirmed to be a critical initiator caspase for receptor-mediated apoptosis signaling in Jurkat cells, since the addition of Ac-IETD-CHO, an inhibitor of caspase-8 and -6, significantly inhibited the death of Jurkat cells by an anti-Fas Ab (Fig. 6A and C). On the other hand, inhibitors for caspase-3 (Ac-DMQD-CHO), caspase-8 and -6 (Ac-IETD-CHO), and caspase-9 (Ac-LEHD-CHO) failed to inhibit CDT-induced apoptosis of Jurkat cells (Fig. 6B and C), suggesting that CDT-induced apoptosis might use a different signaling pathway from that of Fas-mediated apoptosis. To determine which caspase(s) among those we tested is actually involved in CDT-induced apoptosis, we analyzed the effects of inhibitors of caspase-1 (Ac-WEHD-CHO), caspase-2 (Ac-VDVAD-CHO), and caspase-3, -7, and -8 (Ac-DEVD-CHO) on CDT-induced apoptosis. The inhibitor of caspase-1 (Ac-WEHD-CHO) had no inhibitory effect on CDT-induced apoptosis of Jurkat cells at concentrations up to 200 μM. On the other hand, CDT-induced apoptosis was dose dependently inhibited by the inhibitor of caspase-2 (VDVAD) or that of caspase-3, -7, and -8 (DEVD) (Fig. 7A and B). However, the combination of inhibitors of caspase-2 (VDVAD) and of caspase-3, -7, and -8 (DEVD) did not show any multiplier effect (Fig. 7C). Together with the fact that inhibitors of caspase-3 (Ac-DMQD-CHO) and caspase-8 and -6 (Ac-IETD-CHO) failed to prevent CDT-induced apoptosis (Fig. 6), our results strongly suggested

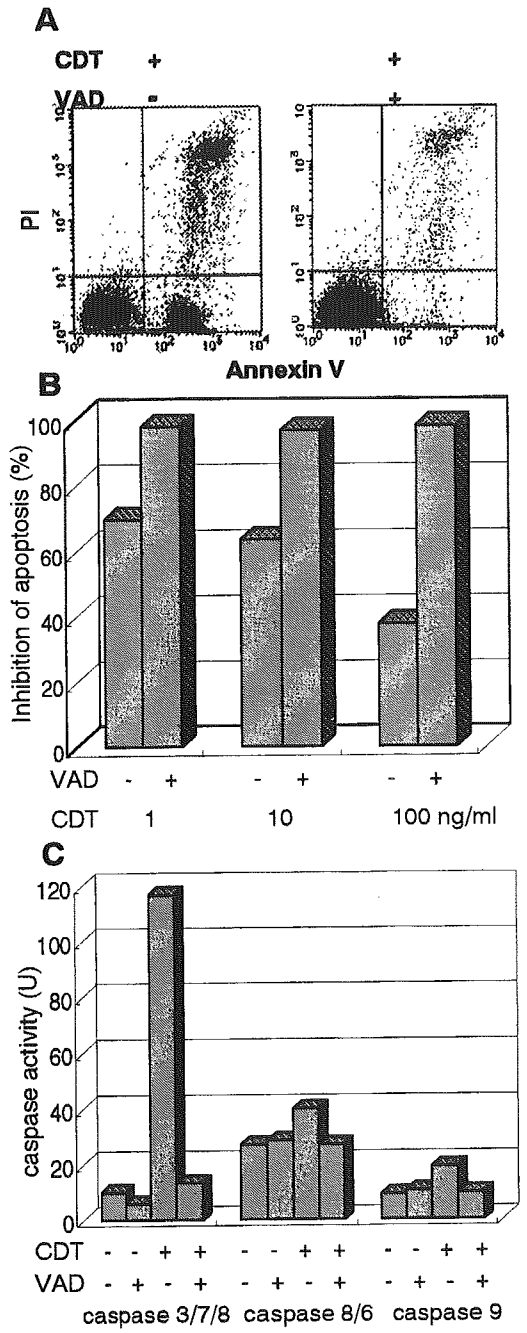

FIG. 5. Effect of general caspase inhibitor on CDT-induced apoptosis. (A) Jurkat cells were preincubated with z-VAD-fmk (100 μM) for 30 min and then were treated with CDT (1, 10, or 100 ng/ml) for 16 h. Cells were stained with FITC-annexin V and PI and analyzed by flow cytometry. The flow cytometry pattern represents CDT (100 ng/ml)-treated lymphocytes with (+) or without (−) z-VAD-fmk. Inhibition of apoptosis was calculated as the relative percentage of living cells, or the population in the LL quadrant (annexin V^- PI^- population). (B) z-VAD-fmk inhibits apoptosis in the cells treated with various concentrations of CDT. (C) Effect of z-VAD-fmk on caspase-3, -7, and -8, caspase-8 and -6, and caspase-9 activity induced by CDTB. Jurkat cells were preincubated with z-VAD-fmk (100 μM) for 30 min and then were treated with CDT (100 ng/ml). Caspase activity was measured as described in Materials and Methods.

that caspase-2 and -7 were mainly involved in the activation of this caspase-dependent apoptotic cascade. We therefore measured the activities of caspase-2 and -7 after CDT treatment for 16 h. To measure caspase-7 activity, we used Ac-DQTD-AMC (substrate for caspase-3 and -7) as a substrate because no caspase-7-specific substrate was available. As shown in Fig. 8A, CDT significantly induced the activation of caspase-2. CDT also induced caspase-3 and -7 activity, but the caspase-3-specific inhibitor Ac-DMQD-CHO did not inhibit the activity at all (Fig. 8A). This clearly indicated that the CDT treatment activated caspase-7. These data suggest that caspase-2 and caspase-7 are really involved in the pathway of CDT-induced apoptotic cell death. It is noteworthy that Ac-VDVAD-CHO (caspase-2 inhibitor) showed an inhibitory effect on caspase-3 and -7 activity. Similarly, Ac-DQTD-CHO (the caspase-3 and -7 inhibitor) clearly inhibited the effect on caspase-2. These results suggest that the caspase-2 and -7 pathways of CDT-induced apoptosis are tightly linked to each other, and they are quite consistent with the results of the experiment on the combination effect of inhibitors of caspase-2 and caspase-3, -7, and -8 (Fig. 7C). The incomplete inhibition of caspase-2 activity by Ac-VDVAD-CHO (caspase-2 inhibitor) implies that another molecule with proteolytic activity similar to that of caspase-2 may be involved in CDT-induced cell death.

To determine whether the mitochondrial pathway is really involved in CDT-induced apoptosis, we analyzed the release of cytochrome *c* from mitochondria in CDT-treated cells. As shown in Fig. 8B, the immunoblotting assay revealed that cytochrome *c* was detectable in the cytosol at 8 h, and more apparently so at 16 h, after CDT treatment of Jurkat cells. The appearance of cytochrome *c* accorded well with the time course of caspase activation, suggesting that the mitochondrial pathway is also involved in CDT-induced apoptosis.

DISCUSSION

In order to investigate CDT-induced apoptosis, we first attempted to establish a cell line model of it. Cytological and biological characterizations of CDT-treated Jurkat and MOLT-4 cells satisfied the apoptosis criteria, such as an increase in membrane conformational changes detected by an increase in the annexin V-positive cell population, intranucleosomal DNA fragmentation, chromatin condensation, and an increase in caspase activity (Fig. 1 to 4). It is noteworthy that the elevation of caspase activity in Jurkat and MOLT-4 cells showed some considerable differences in time course and in activation pattern: the culmination of induced caspase activity was higher in CDT-treated MOLT-4 cells than in similarly treated Jurkat cells. This may suggest that Jurkat and MOLT-4 cells took different apoptotic pathways after exposure to CDT. In this context, it should be noted that Jurkat, but not MOLT-4, cells are deficient in p53 (10). p53 is implicated in the G_2/M block in CDT-treated keratinocytes and fibroblasts (7). The phosphorylation of p53 and other phosphorylation signals could play some role in CDT-induced apoptosis, and the lack of p53 might alter the pathway of apoptosis of Jurkat cells from that of MOLT-4 cells.

We tried to obtain further insights into the understanding of the signaling pathway of CDT-induced apoptosis, especially regarding the caspase cascade(s). Caspases are members of the

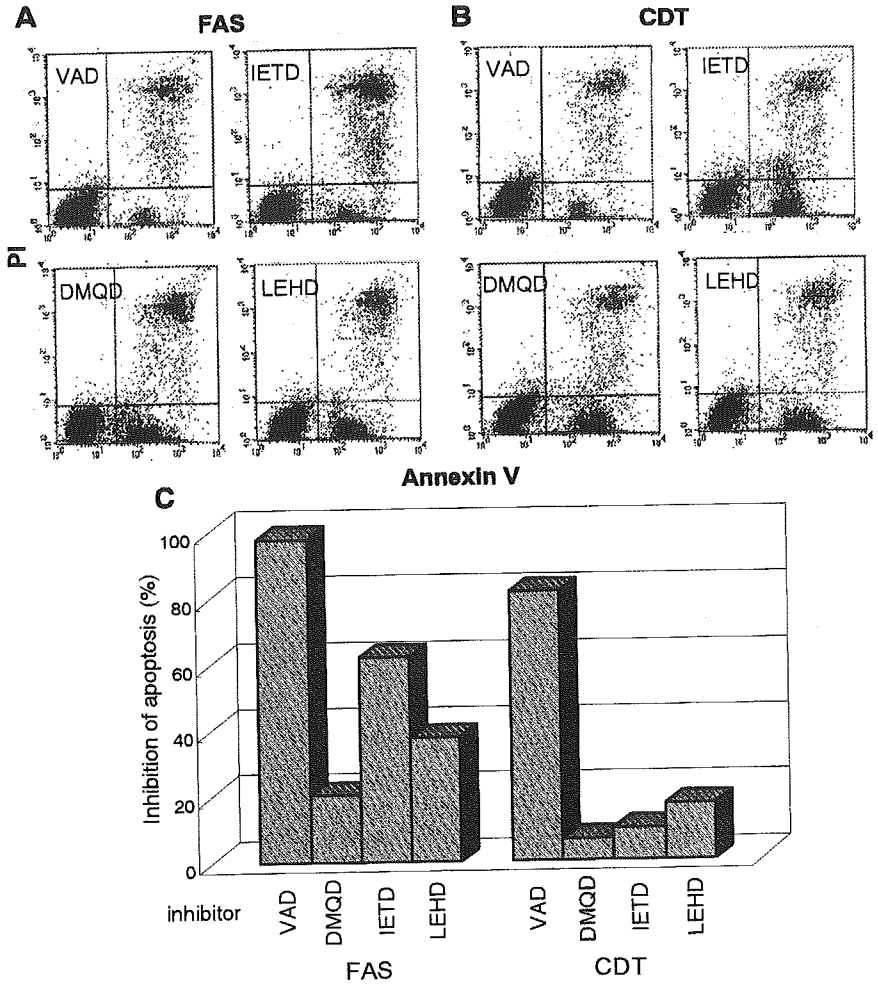

FIG. 6. Effect of various caspase inhibitors on CDT-induced apoptosis. Jurkat cells were preincubated with the indicated inhibitors (100 μM) for 30 min and then were treated with anti-Fas Ab (100 ng/ml) (A) or CDT (100 ng/ml) (B). After 16 h, cells were stained with FITC-annexin V and PI and analyzed by FACScan. The inhibitors used were VAD (general caspase inhibitor), DMQD (caspase-3 inhibitor), IETD (caspase-8 and -6 inhibitor), and LEHD (caspase-9 inhibitor). (A and B) Representative flow cytometry patterns. (C) Effect of caspase inhibitors on apoptosis induced by anti-Fas Ab (left) or CDT (right). Inhibition of apoptosis was defined as the relative percentage of normal living cells (annexin V^- PI^-).

aspartate-specific cysteine protease family which play a critical role in apoptosis (6, 39). They are composed of two major subfamilies, initiator caspases and effector caspases, based on the presence or absence of a large prodomain in the amino-terminal region (33). Initiator caspases generally act upstream of the proteolytic cascade, while effector caspases act downstream and are involved in the cleavage of specific cellular substrate proteins (41). Once processed, the substrates induce morphological changes characteristic of the apoptotic process (8, 11). The long prodomains of the initiator caspases trigger and/or facilitate the activation of proenzymes through interactions with adaptor molecules (13). Caspase-2, -8, -9, and -10 generally act as initiator caspases upstream of the cascade of effector caspases with small prodomains, such as caspase-3, -6, and -7 (26). Among the caspases, caspase-8, -9, and -10 play a fundamental role in transducing the specific apoptotic signal, and they cleave and activate effector procaspase-3, -6, and -7 (4). Effector caspases, in turn, cleave various proteins, leading to morphological and biochemical features characteristic of apoptosis. Recently, it has become clear that caspase-9 is involved in the apoptotic pathway that relys on mitochondrial dysfunction (15). Caspase-8 and -10 are involved in the apoptosis pathway mediated by death receptors (2).

Our results indicated that inhibitors of caspase-2 and -7 showed inhibitory effects on CDT-induced apoptosis. Several bacterial toxins are known to induce apoptosis through caspase-dependent pathways, although the exact molecular mechanism of the signaling cascade has not been well characterized. For instance, Shiga toxin and Shiga-like toxin have been demonstrated to activate caspase-2, -3, -6, -8, and -9 (5, 17, 18). It was suggested that these toxins use the caspase cascade involved in Fas-mediated apoptosis. Other toxins, such as *E. coli* heat-labile enterotoxin (32), *Clostridium difficile* toxin B (29), diphtheria toxin (19), and *Mannheimia haemolytica* leukotoxin (23), were shown to induce caspase-3. However, a detailed caspase cascade induced by bacterial toxins has not been well established. To our knowledge, this is the first report that a bacterial toxin preferentially utilizes caspase-2 and -7 in

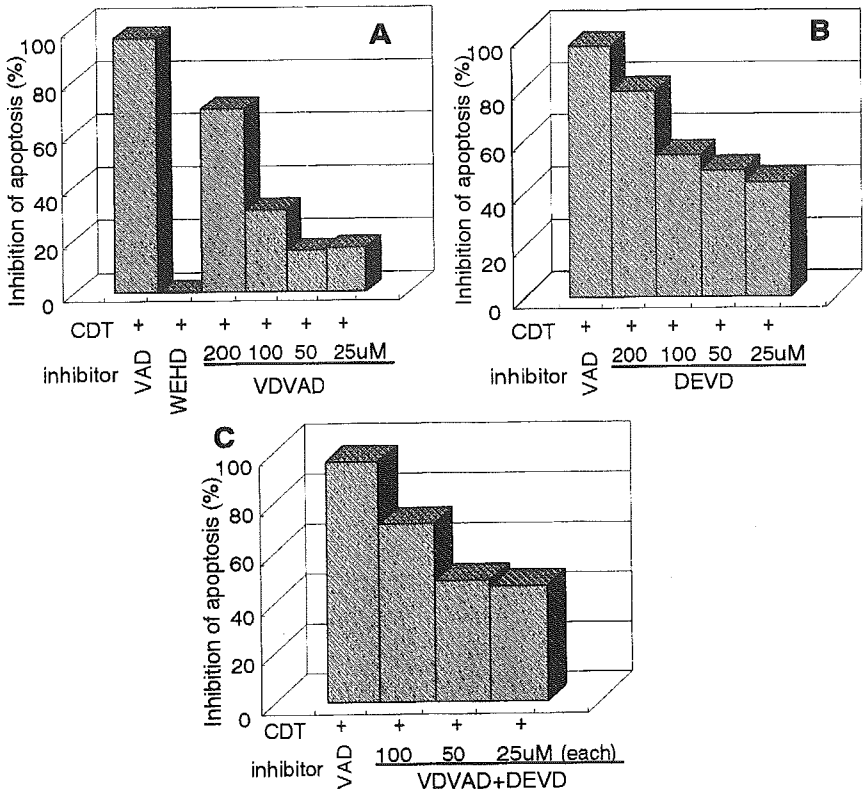

FIG. 7. Dose-dependent inhibitory effects of caspase inhibitors on CDT-induced apoptosis. Jurkat cells were preincubated with various concentrations of caspase inhibitors (25, 50, 100, and 200 μM) for 30 min and then were treated with CDT (100 ng/ml). The inhibitors used were WEHD (caspase-1 inhibitor), VDVAD (caspase-2 inhibitor), and DEVD (caspase-3, -7, and -8 inhibitor). After 16 h, cells were stained with FITC-annexin V and PI and analyzed by flow cytometry. Panels show the relative inhibition of CDT-induced apoptosis with VDVAD (A), DEVD (B), and VDVAD and DEVD (C). Inhibition of apoptosis was defined as the relative percentage of living cells (annexin V^- PI^-). VAD (general caspase inhibitor) and WEHD were used at concentrations of 100 and 200 μM, respectively.

the signaling pathway for apoptosis. In recent studies, caspase-2 was implicated in the release of cytochrome *c* from mitochondria in stress-induced apoptotic pathways (16, 22, 27, 30). One such stress-inducing agent is a topoisomerase II poison, etoposide, that induces double-stranded DNA breaks in cells. Robertson et al. (30) demonstrated that etoposide-induced DNA damage induces activation of caspase-2 and hence results in cytochrome *c* release from mitochondria and subsequent apoptosis. It is interesting that a possible mechanism by which CDT can induce cytopathic effects involves DNA strand breaks induced by its putative DNase activity (12, 20). Such CDT-induced DNA damage may trigger the mitochondrial cascade including caspase-2 and -7. A recent report has indicated the requirement of caspase-2 for the initiation of stress-induced apoptosis prior to mitochondrial permeabilization (22). In our case, CDT-induced DNA damage may directly activate caspase-2 and then induce the mitochondrial cascade, probably followed by caspase-7 activation. Caspase-7 is a late signal transducer and one of the members of the apoptosome complex which is activated by mitochondrial stress (3). Both caspase-2 and -7 are involved in stress-induced cascades, suggesting that CDT-induced apoptosis is related to the mitochondrial pathway. Our present results indicate that CDT can induce mitochondrial membrane permeabilization, resulting in the release of cytochrome *c*, and that this mitochondrial pathway is highly involved in CDT-induced apoptosis. This is quite in agreement with an experiment showing that Bcl-2 overexpression reduces apoptosis in a CDT-treated human B lymphoblastoid cell line, JY (35).

Fas ligation on the cell surface induces apoptosis through the receptor-mediated signaling pathway, which involves caspase-8 as an initiation signal (2). The fact that caspase-8 inhibitor blocked Fas-mediated apoptosis in Jurkat cells (Fig. 6) indicated that the Fas-dependent apoptotic pathway was active in this cell line. In contrast, no inhibitory effect of caspase-8 inhibitor on CDT-induced apoptosis was observed in Jurkat cells, suggesting that the cytotoxic effect of CDT does not require the activation of death receptors on the cell surface.

Since CDT is able to induce apoptosis of activated T cells, this toxin may play an important role in that the bacteria evade T-cell immune responses in the periodontal pocket. It is conceivable that CDT produced by this pathogen exacerbates local inflammation by inducing apoptotic cell death of T lymphocytes that are responsible for the clearance of bacteria from the periodontal pocket. Further studies on the effect of CDT on the caspase network should unveil the CDT-related signal transduction pathway in T-lymphocyte apoptosis that may lead to the suppression of immune responses to the pathogen.

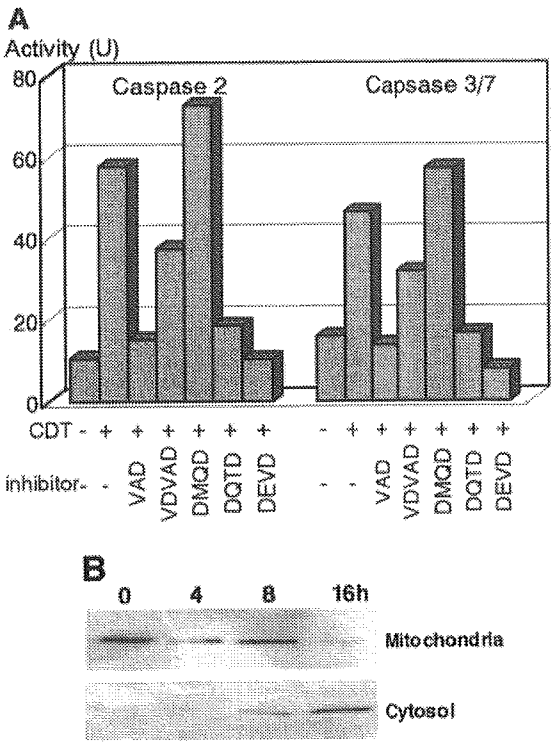

FIG. 8. Elevation of caspase-2 or -7 activity and cytochrome *c* release by CDT treatment. (A) Jurkat cells were preincubated with the indicated inhibitor (100 μM) for 30 min and then were treated with CDT (100 ng/ml) for 16 h. The inhibitors used were VAD (general caspase inhibitor), VDVAD (caspase-2 inhibitor), DMQD (caspase-3 inhibitor), DQTD (caspase-3 and -7 inhibitor), and DEVD (caspase-3, -7, and -8 inhibitor). Caspase activity was measured as described in Materials and Methods. (B) Cytosol and mitochondrial fractions were extracted from Jurkat cells that were treated with CDT (100 ng/ml) for 0, 4, 8, and 16 h and were subsequently immunoblotted with an anti-cytochrome *c* Ab followed by a horseradish peroxidase-conjugated secondary Ab. The bands of cytochrome *c* were visualized by ECL.

ACKNOWLEDGMENTS

We thank Kei Nakachi, Donald G. MacPhee, and Seishi Kyoizumi at the Department of Radiobiology and Molecular Epidemiology, Radiation Effects Research Foundation, for helpful suggestions. We thank the Research Facilities, Hiroshima University School of Dentistry and School of Medicine, for the use of facilities.

This study was supported in part by a Grant for Development of Highly Advanced Medical Technology (A) and by a Grant-in-Aid for Scientific Research (B) from the Ministry of Education, Science, Sports and Culture of Japan.

REFERENCES

1. **Alby, F., R. Mazars, J. De Rycke, E. Guillou, V. Baldin, J.-M. Darbon, and B. Ducommun.** 2001. Study of the cytolethal distending toxin (CDT)-activated cell cycle checkpoint. Involvement of the CHK2 kinase. FEBS Lett. **491:**261–265.
2. **Ashkenazi, A., and V. M. Dixit.** 1998. Death receptors: signaling and modulation. Science **281:**1305–1308.
3. **Bratton, S. B., M. Macfarlane, K. Cain, and G. M. Cohen.** 2000. Protein complexes activate distinct caspase cascades in death receptor and stress induced apoptosis. Exp. Cell Res. **256:**27–33.
4. **Budihardjo, I., H. Oliver, M. Lutter, X. Luo, and X. Wang.** 1999. Biochemical pathways of caspase activation during apoptosis. Annu. Rev. Cell Dev. Biol. **15:**269–290.
5. **Ching, J. C., N. L. Jones, P. J. Ceponis, M. A. Karmali, and P. M. Sherman.** 2002. *Escherichia coli* Shiga-like toxins induce apoptosis and cleavage of poly(ADP-ribose) polymerase via in vitro activation of caspases. Infect. Immun. **70:**4669–4677.
6. **Cohen, G. M.** 1997. Caspases: the executioners of apoptosis. Biochem. J. **326:**1–16.
7. **Cortes-Bratti, X., C. Karlsson, T. Lagergard, M. Thelestam, and T. Frisan.** 2001. The *Haemophilus ducreyi* cytolethal distending toxin induces cell cycle arrest and apoptosis via the DNA damage checkpoint pathways. J. Biol. Chem. **276:**5296–5302.
8. **Cryns, V., and J. Yuan.** 1998. Proteases to die for. Genes Dev. **12:**1551–1570.
9. **Deng, K., J. L. Latimer, D. A. Lewis, and E. J. Hansen.** 2001. Investigation of the interaction among the components of the cytolethal distending toxin of *Haemophilus ducreyi*. Biochem. Biophys. Res. Commun. **20:**609–615.
10. **Dreyfus, D. H., M. Nagasawa, C. A. Kelleher, and E. W. Gelfand.** 2000. Stable expression of Epstein-Barr virus BZLF-1-encoded ZEBRA protein activates p53-dependent transcription in human Jurkat T-lymphoblastoid cells. Blood **96:**625–634.
11. **Earnshaw, W. C., L. M. Martins, and S. H. Kaufmann.** 1999. Mammalian caspases: structure, activation, substrates, and functions during apoptosis. Annu. Rev. Biochem. **68:**383–424.
12. **Elwell, C. A., K. Chao, K. Patel, and L. A. Dreyfus.** 2001. *Escherichia coli* CdtB mediates cytolethal distending toxin cell cycle arrest. Infect. Immun. **69:**3418–3422.
13. **Fesik, S. W.** 2000. Insights into programmed cell death through structural biology. Cell **103:**273–282.
14. **Frisk, A., M. Labens, C. Johansson, H. Ahmed, L. Svensson, K. Ahlman, and T. Lagergard.** 2001. The role of different protein components from the *Haemophilus ducreyi* cytolethal distending toxin in the generation of cell toxicity. Microb. Pathog. **30:**313–324.
15. **Green, D. R.** 2000. Apoptotic pathways: paper wraps stone blunts scissors. Cell **102:**1–4.
16. **Guo, Y., S. M. Srinivasula, A. Druilhe, T. Fernandes-Alnemri, and E. S. Alnemri.** 2002. Caspase-2 induces apoptosis by releasing proapoptotic proteins from mitochondria. J. Biol. Chem. **277:**13430–13437.
17. **Kiyokawa, N., T. Mori, T. Taguchi, M. Saito, K. Mimori, T. Suzuki, T. Sekino, N. Sato, H. Nakajima, Y. U. Katagiri, T. Takeda, and J. Fujimoto.** 2001. Activation of the caspase cascade during Stx-1-induced apoptosis in Burkitt's lymphoma cells. J. Cell. Biochem. **81:**128–142.
18. **Kojio, S., H. Zhang, M. Ohmura, F. Gondaira, N. Kobayashi, and T. Yamamoto.** 2000. Caspase-3 activation and apoptosis induction coupled with the retrograde transport of Shiga toxin: inhibition by brefeldin A. FEMS Immunol. Med. Microbiol. **29:**275–281.
19. **Komatsu, N., T. Oda, and T. Muramatsu.** 1998. Involvement of both caspase-like proteases and serine proteases in apoptotic cell death induced by ricin, modeccin, diphtheria toxin, and pseudomonas toxin. J. Biochem. (Tokyo) **124:**1038–1044.
20. **Lara-Tejero, M., and J. E. Galan.** 2000. A bacterial toxin that controls cell cycle progression as a deoxyribonuclease I-like protein. Science **290:**354–357.
21. **Lara-Tejero, M., and J. E. Galan.** 2001. CdtA, CdtB, and CdtC form a tripartate complex that is required for cytolethal distending toxin activity. Infect. Immun. **69:**4358–4365.
22. **Lassus, P., X. Opitz-Araya, and Y. Lazebnik.** 2002. Requirement for caspase-2 in stress-induced apoptosis before mitochondrial permeabilization. Science **297:**1352–1354.
23. **Leite, F., S. O'Brien, M. J. Sylte, T. Page, D. Atapattu, and C. J. Czuprynski.** 2002. Inflammatory cytokines enhance the interaction of *Mannheimia haemolytica* leukotoxin with bovine peripheral blood neutrophils in vitro. Infect. Immun. **70:**4336–4343.
24. **Lewis, D. A., M. K. Stevens, J. L. Latimer, C. K. Ward, K. Deng, R. Blick, S. R. Lumbley, C. A. Ison, and E. J. Hansen.** 2001. Characterization of *Haemophilus ducreyi cdtA*, *cdtB*, and *cdtC* mutants in in vitro and in vivo systems. Infect. Immun. **69:**5626–5634.
25. **Mangan, D. F., N. S. Taichman, E. T. Lally, and S. M. Wahl.** 1991. Lethal effects of *Actinobacillus actinomycetemcomitans* leukotoxin on human T lymphocytes. Infect. Immun. **59:**3267–3272.
26. **Nicholson, D. W., and N. A. Thornberry.** 1997. Caspases: killer proteases. Trends Biochem. Sci. **22:**299–306.
27. **Paroni, G., C. Henderson, C. Schneider, and C. Brancolini.** 2002. Caspase-2 can trigger cytochrome *c* release and apoptosis from the nucleus. J. Biol. Chem. **277:**15147–15161.
28. **Pickett, C. L., and C. A. Whitehouse.** 1999. The cytolethal distending toxin family. Trends Microbiol. **7:**292–297.
29. **Qa'Dan, M., M. Ramsey, J. Daniel, L. M. Spyres, B. Safiejko-Mroczka, W. Ortiz-Leduc, and J. D. Ballard.** 2002. *Clostridium difficile* toxin B activates dual caspase-dependent and caspase-independent apoptosis in intoxicated cells. Cell. Microbiol. **4:**425–434.
30. **Robertson, J. D., M. Enoksson, M. Suomela, B. Zhivotovsky, and S. Orrenius.** 2002. Caspase-2 acts upstream of mitochondria to promote cytochrome *c* release during etoposide-induced apoptosis. J. Biol. Chem. **277:**29803–29809.
31. **Saiki, K., K. Konishi, T. Gomi, T. Nishihara, and M. Yoshikawa.** 2001. Reconstitution and purification of cytolethal distending toxin of *Actinobacillus actinomycetemcomitans*. Microbiol. Immunol. **45:**497–506.
32. **Salmond, R. J., R. S. Pitman, E. Jimi, M. Soriani, T. R. Hirst, S. Ghosh, M. Rincon, and N. A. Williams.** 2002. $CD8^+$ T cell apoptosis induced by *Esch-*

erichia coli heat-labile enterotoxin B subunit occurs via a novel pathway involving NF-kappaB-dependent caspase activation. Eur. J. Immunol. **32:** 1737–1747.

33. **Salvesen, G. S., and V. M. Dixit.** 1999. Caspase activation: the induced-proximity model. Proc. Natl. Acad. Sci. USA **96:**10964–10967.
34. **Shenker, B. J., R. H. Hoffmaster, T. L. Mckay, and D. R. Demuth.** 2000. Expression of the cytolethal distending toxin (Cdt) operon in *Actinobacillus actinomycetemcomitans*: evidence that the CdtB protein is responsible for G_2 arrest of the cell cycle in human T cells. J. Immunol. **165:**2612–2618.
35. **Shenker, B. J., R. H. Hoffmaster, A. Zekavat, N. Yamaguchi, E. T. Lally, and D. Demuth.** 2001. Induction of apoptosis in human T cells by *Actinobacillus actinomycetemcomitans* cytolethal distending toxin is a consequence of G_2 arrest of the cell cycle. J. Immunol. **167:**435–441.
36. **Shenker, B. J., T. McKay, S. Datar, M. Miller, R. Chowhan, and D. Demuth.** 1999. *Actinobacillus actinomycetemcomitans* immunosuppressive protein is a member of the family of cytolethal distending toxins capable of causing a G_2 arrest in human T cells. J. Immunol. **162:**4773–4780.
37. **Shenker, B. J., L. Vitale, and C. King.** 1995. Induction of human T cells that coexpress CD4 and CD8 by an immunomodulatory protein produced by *Actinobacillus actinomycetemcomitans*. Cell. Immunol. **164:**36–46.
38. **Slots, J., H. S. Reynolds, and R. J. Genco.** 1980. *Actinobacillus actinomycetemcomitans* in human periodontal disease: a cross-sectional microbiological investigation. Infect. Immun. **29:**1013–1020.
39. **Stennicke, H. R., and G. S. Salvesen.** 1997. Biochemical characteristics of caspases-3, -6, -7, and -8. J. Biol. Chem. **272:**25719–25723.
40. **Sugai, M., T. Kawamoto, S. Y. Peres, Y. Ueno, H. Komatsuzawa, T. Fujiwara, H. Kurihara, H. Suginaka, and E. Oswald.** 1998. The cell cycle-specific growth-inhibitory factor produced by *Actinobacillus actinomycetemcomitans* is a cytolethal distending toxin. Infect. Immun. **66:**5008–5019.
41. **Thornberry, N. A., and Y. Lazebnik.** 1998. Caspases: enemies within. Science **281:**1312–1316.

Editor: V. J. DiRita

Histochem Cell Biol (2004) 121:291–297
DOI 10.1007/s00418-004-0636-6

ORIGINAL PAPER

Mutsumi Miyauchi · Shoji Kitagawa · Masae Hiraoka · Akihisa Saito · Sunao Sato · Yasusei Kudo · Ikuko Ogawa · Takashi Takata

Immunolocalization of CXC chemokine and recruitment of polymorphonuclear leukocytes in the rat molar periodontal tissue after topical application of lipopolysaccharide

Accepted: 5 February 2004 / Published online: 24 March 2004

Abstract This study investigated the recruitment of polymorphonuclear leukocytes (PMNs) and the immunolocalization of CXC chemokines, including macrophage inflammatory protein-2 (MIP-2) and cytokine-induced neutrophil chemoattractant-2 (CINC-2) in rat periodontal tissue after topical application of lipopolysaccharide (LPS; 5 mg/ml) from *Escherichia coli* into the rat molar gingival sulcus. In normal periodontal tissues, a small number of MIP-2- and CINC-2-positive cells were seen in junctional epithelium (JE), especially in its coronal half. After topical application of LPS, a prominent increase of MIP-2- and CINC-2-positive JE cells was observed. Almost all JE cells strongly expressed them at day 1 and day 2, and then the number of chemokine-positive cells returned to normal at day 7. Corresponding to these chemokine expressions, LPS application induced a significant increase in the number of PMNs in the sub-JE area from 1 h to 2 days and a significant increase in JE area from 3 h to 5 days, indicating a dynamic flow of PMNs from the sub-JE area into JE. These findings indicated that JE cells produced MIP-2 and CINC-2 in response to LPS stimulation and suggested that MIP-2 and CINC-2 may be responsible for PMN migration toward the periodontal pathogen and may play an important role in the initiation of inflammation and subsequent periodontal tissue destruction.

M. Miyauchi · S. Kitagawa · M. Hiraoka · A. Saito · S. Sato · Y. Kudo · T. Takata (✉)
Department of Oral Maxillofacial Pathobiology,
Division of Frontier Biomedical Science,
Graduate School of Biomedical Sciences,
Hiroshima University,
1-2-3 Kasumi, Minami-ku, 734-8553 Hiroshima, Japan
e-mail: ttakata@hiroshima-u.ac.jp
Tel.: +81-82-2575634
Fax: +81-82-2575619

I. Ogawa · T. Takata
Center of Oral Clinical Examination,
Hiroshima University Hospital,
1-2-3 Kasumi, Minami-ku, 734-8553 Hiroshima, Japan

Keywords Chemokine · Lipopolysaccharide · Polymorphonuclear leukocyte · Periodontitis · Animal study

Introduction

Superficial periodontal tissues are constantly exposed to plaque-associated bacteria and bacterial lipopolysaccharides (LPS), which can induce an inflammatory reaction and consequent tissue destruction (Socransky and Haffajee 1992; Wilson et al. 1996). Inflammation is an essential component of the host defense response to bacterial challenge, and the migration of polymorphonuclear leukocytes (PMNs) from blood vessel into gingival tissues is a critical part of the initial inflammatory responses (Liu 2001). The gingival epithelium consists of three different compartments, oral gingival epithelium (OGE), oral sulcular epithelium (OSE), and junctional epithelium (JE). OGE and OSE are keratinized squamous epithelium and are non-permeable. On the other hand, JE is non-keratinized squamous epithelium, which provides the epithelial attachment to tooth surface. It is quite permeable and serves a pathway for transmigration of PMNs moving toward the gingival sulcus. In fact, many PMNs are present in diseased gingival connective tissue subjacent to the JE and continuously migrate into the gingival sulcus through the JE (Schroeder 1973; Wirthlin and Hussain 1992).

The recruitment of PMNs into the site of bacterial infection results from many processes including activation of capillary loops, adhesion of PMNs to endothelial cells, transendothelial migration, and migration toward the infecting bacteria. Adhesion molecules and chemokines are key mediators for these processes. Chemokines are a family of over 40 small cytokines, which have been isolated by their ability to induce chemotaxis of leukocytes. Chemokines have been classified into four subfamilies depending on the number and spacing of the first conserved cysteine residues in the NH_2 terminal region: CXC, CC, XC, and CX3C. CXC chemokines are low molecular weight proteins, which have been reported to

be the most powerful mediator for selective PMN recruitment and activation. It is well known that interleukin-8 (IL-8) is the most potent human CXC chemokine. IL-8 can be produced by various cells including leukocytes, fibroblasts, endothelial cells, and keratinocytes, in response to both endogenous and exogenous stimuli (Oppenheim et al. 1991; Bickel 1993). In particular, it is upregulated by bacterial LPS and proinflammatory cytokines such as interleukin-1 (IL-1) and tumor necrosis factor-α (TNF-α; Zwahlen et al. 1993). Recent reports had indicated that IL-8 protein and its mRNA were present in human inflamed gingival tissues and that IL-8 protein levels in gingival crevicular fluid (Payme et al. 1993; Gamonal et al. 2000, 2001) and gingival tissue significantly increased in diseased sites and were related to the influx of PMNs (Tonetti et al. 1994, 1995; Tonetti 1997).

In previous studies, we have reported that initial periodontal tissue destruction is provoked by topical application of 5 mg/ml LPS from *Escherichia coli* into the rat gingival sulcus (Ijuhin 1988; Takata et al. 1997; Miyauchi et al. 1998, 2001). In summary, infiltration of numerous PMNs in the JE and sub-JE area (Ijuhin 1988), transient accumulation of exudative macrophages (Miyauchi et al. 1998), vascular dilatation and inflammatory edema in the sub-JE area, enhancement of proliferative activity of JE cells (Takata et al. 1997), and stimulation of osteoclastic bone resorption showing a biphasic response peaking at 3 h and 3 days after LPS treatment (Ijuhin 1988) were observed. Furthermore, we reported transient overexpression of proinflammatory cytokines, namely TNF-α, IL-1α, and IL-1β, in the JE cells with a peak at 3 h and suggested that JE cells may play an important role in the first line of defense against LPS challenge and the following tissue destruction (Miyauchi et al. 2001). Considering the inductive production of IL-8 by these proinflammatory cytokines and a possible role as specific mediator of PMN influx, it is interesting to investigate the relation between the dynamic changes of IL-8 expression in periodontal tissue and PMN migration during an LPS-induced acute inflammatory episode using this animal model. However, the murine counterpart of IL-8 has not been identified yet. It is likely that IL-8 dose not exist in rodents and that other murine CXC chemokines replace IL-8.

In this study, to clarify the critical role of CXC chemokines in PMN recruitment into the periodontal disease site, we investigated the immunolocalization of two important murine CXC chemokines including macrophage inflammatory protein-2 (MIP-2) and cytokine-induced neutrophil chemoattractant-2 (CINC-2) in periodontal tissues after topical application of LPS using a rat animal model and compared the immunolocalization of MIP-2 and CINC-2 with local infiltration of PMNs.

Materials and methods

Animal experiment

A total of 42, seven-week-old (about 190 g), male Wistar rats was used in this study. They were divided into seven groups of six rats each. Under intraperitoneal anesthesia of 20% ethyl carbamate (100 mg/100 g body weight), a rat was fixed on its back on an experimental stand. A cotton roll (2 mm in diameter and 1 cm in length) saturated with 5 mg/ml LPS from *Escherichia coli* (Sigma, St. Louis, MO, USA) in sterile physiological saline (Otsuka, Tokyo, Japan) was placed on the occlusal surface of the right and left upper molar regions for 1 h. The cotton roll was changed every 20 min. Rats were killed at 1 and 3 h, and 1, 2, 3, and 7 days after the LPS treatment, six at each time, by an overdose of ethyl ether. The remaining six rats were used as an untreated control group.

The experimental protocol was approved by the animal care committee of Hiroshima University.

Tissue samples were resected *en bloc* from the right and left upper molar regions and fixed for 8 h in a periodic-lysine paraformaldehyde solution at 4°C. The samples were cut into two parts, which included the first or second molar (about 2 mm thick), at the buccopalatal plane parallel to each distopalatal root. They were then decalcified in a 10% ethylenediaminetetraacetate (EDTA) solution in phosphate-buffered saline (PBS; pH 7.4) for 5 days at 4°C. The decalcified tissue blocks were embedded in OCT compound (Tissue Tec; Miles, Naperville, IL, USA). Serial frozen sections (8 μm thick) parallel to the long axis of the tooth, including the root apex were cut and collected on glass slides.

Polyclonal antibodies

The CL95575AP polyclonal antibody (Cedarlane Laboratories, Ontario, Canada) was employed to detect rat MIP-2. Rat CINC-2 was identified with the anti-rat GRO/CINC-2α, 2β rabbit IgG (IBL, Fujioka, Japan), which was produced using highly purified recombinant peptide for the common N-terminal region of rat GRO/CINC-2α, 2β and did not show crossreactivity with rat GRO/CINC-1 and MIP-2.

Immunohistochemistry

The following immunostaining was carried out using a Dako-LSB2 kit (Dako, Carpinteria, CA, USA). After washing in PBS each section was incubated with normal goat serum for 30 min at 4°C and then incubated with polyclonal antibodies to CXC chemokines for 24 h at 4°C in a humid atmosphere. Polyclonal antibodies to MIP-2 and CINC-2 were diluted in 0.001 M PBS containing 5% normal rat serum to 1:100 and 1:500, respectively. After being rinsed with PBS the sections were incubated with biotinylated rabbit anti-mouse IgG serum containing 5% normal rat serum for 30 min. The sections were rinsed in PBS and immersed in 0.3% hydrogen peroxide in PBS to block the endogenous peroxidase activity for 1 h. The sections were rinsed with PBS, incubated with the peroxidase-conjugated streptavidin for 30 min and then rinsed with PBS again. The color was developed with 0.025% 3,3′-diaminobenzidine tetrahydrochloride in TRIS-HCl buffer plus hydrogen peroxide (Kyowa Medics, Tokyo, Japan). The specimens were counterstained with Mayer's hematoxylin, dehydrated, and then mounted.

Specificity was ascertained by substituting PBS and normal rabbit serum for each antibody.

Histometric analysis of PMN infiltration

The number of PMNs infiltrated into the JE (JE area) and gingival connective tissue subjacent to the JE (sub-JE area) was statistically analyzed. For the morphometric analysis, the number of PMNs in the JE area and sub-JE area was counted using specimens stained

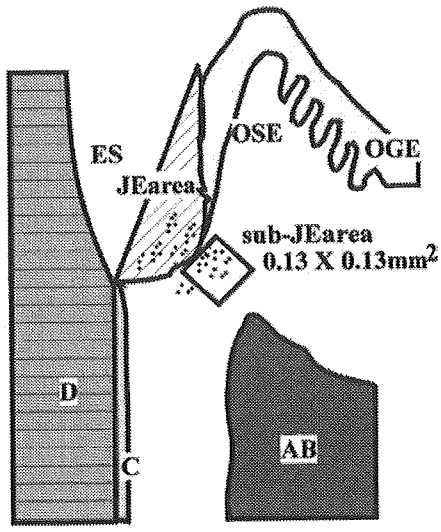

Fig. 1 A diagram illustrating the two areas used for counting the number of polymorphonuclear leukocytes (PMNs): (1) *JE area* all PMNs in the JE were counted; (2) *sub-JE area* PMNs seen in a 0.13×0.13 mm^2 connective tissue area subjacent to JE near the contact point of JE and OSE at the basal cell layer. *AB* Alveolar bone, *C* cementum, *ES* enamel space, *OGE* oral gingival epithelium, *OSE* oral sulcular epithelium, *JE* junctional epithelium, *D* dentin

with hematoxylin and eosin. The small round cells having a nucleus with three to five lobes were judged as PMNs. On average, we counted the number of PMNs at 20 different sites in each experimental and control group. The two counting areas are illustrated in Fig. 1:

1. PMNs in JE area: the palatal gingival tissue of each selected specimen was photographed under a magnification of ×33. On the color prints (enlarged to a final magnification of ×180), the number of PMNs seen in the JE area was counted. After tracing the JE area on translucent paper using the same prints, the JE area traced was measured by the LA 500 image analysis system (PIAS, Osaka, Japan). The number of PMNs in a unit area (1 mm^2) was calculated.
2. PMNs in sub-JE area: using the same specimen, PMNs infiltrated in a 0.13×0.13 mm^2 connective tissue area subjacent to JE were counted under a light microscope equipped with an ocular micrometer, and the number of PMNs seen in a unit area (1 mm^2) was also calculated. The results were shown as mean±SE. According to Fisher's system, the mean values obtained were analyzed for statistical differences using Wilcoxon's test for non-paired examination.

Results

Histological findings

In the normal gingival tissue of untreated control rats, the JE showed minimal migration of PMNs through intercellular spaces. In the connective tissue area subjacent to the JE, a small number of PMNs was seen but no obvious inflammatory changes were observed (Fig. 2A). LPS application caused edematous changes, dilatation of blood capillaries, and infiltration of PMNs into the gingival connective tissue subjacent to the JE. Numerous PMNs migrated into the enlarged intercellular spaces of the JE (Fig. 2B), especially at day 1 and day 2. These findings have appeared in 1-h specimens and persisted until 5 days after LPS application. In the case with severe intra-JE infiltration of PMNs, initial pocket formation was seen associated with JE cell damage by PMNs. The inflammatory changes gradually decreased with time and disappeared by day 7.

Neither lateral JE nor apical migration of the JE was seen throughout the experimental periods.

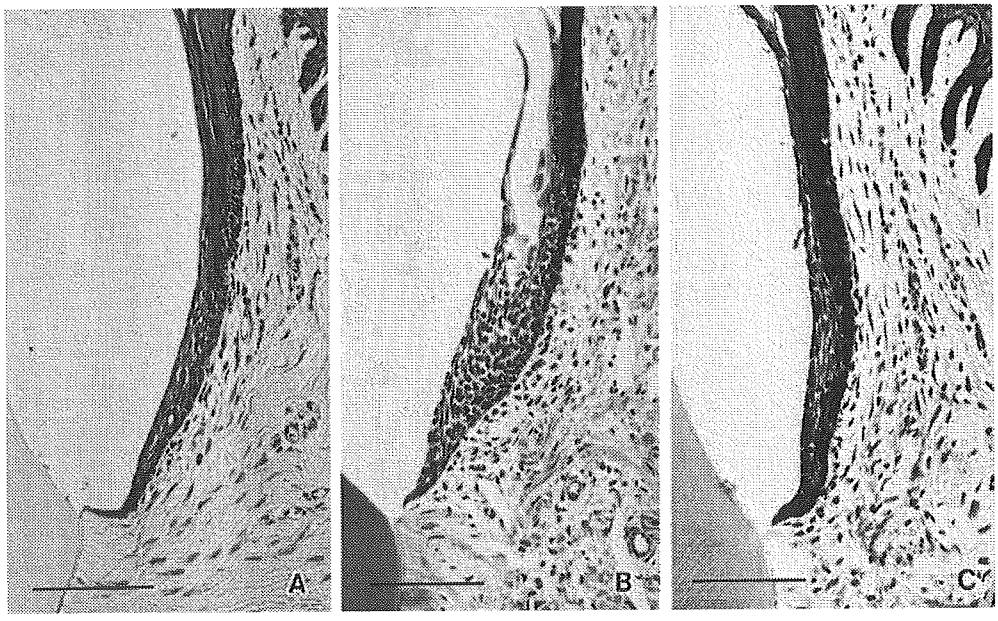

Fig. 2A–C Histological findings in gingival tissues of untreated control animal (**A**), and 3 h (**B**) and 7 days (**C**) after lipopolysaccharide (LPS) application. **A** A small number of PMNs was observed in junctional epithelium (JE). **B** Numerous PMNs migrated into the elongated intercellular spaces of JE cells. **C** The number of PMNs was reduced to normal level. *Scale bars* 0.1 mm (×150; H&E stain)

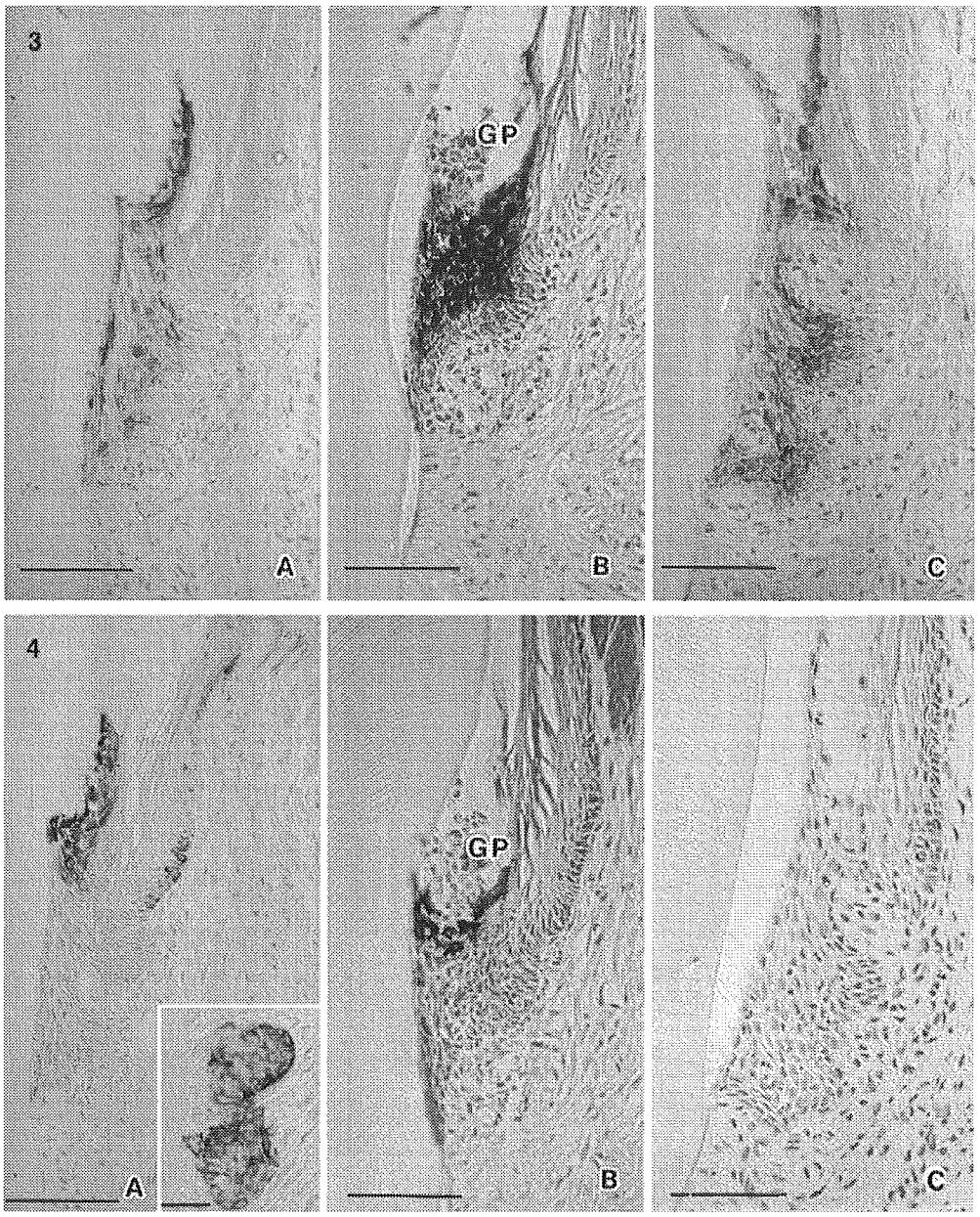

Fig. 3A–C Immunohistochemical staining of macrophage inflammatory protein-2 (MIP-2) in the gingival tissues of untreated control animal (**A**), and 1 day (**B**) and 3 days (**C**) after LPS application. **A** Positive staining is partially seen in the JE cells. **B** Almost all JE cells are strongly positive for MIP-2. PMNs infiltrated into the gingival pocket, JE, and gingival connective tissue adjacent to JE show weakly positive staining. *GP* Gingival pocket. **C** Number of MIP-2-positive cells are remarkably decreased. *Scale bars* 0.1 mm (×150; SAB method)

Fig. 4A–C Immunohistochemical staining of cytokine-induced neutrophil chemoattractant-2 (CINC-2) in the gingival tissues of untreated control animal (**A**), and 1 day (**B**) and 3 days (**C**) after LPS application. **A** JE cells in their coronal parts were strongly positive for CINC-2. Several CINC-2-positive basal cells are seen in the OSE. Epithelial remnants of Malassez show intense staining of CINC-2 (*inset*). **B** JE cells in their coronal parts are still strongly positive for CINC-2. Several JE cells in the apical part and PMNs were also weakly positive for CINC-2. *GP* Gingival pocket. **C** Positive reaction in gingival tissue is not detected. *Scale bars* **A–C** 0.1 mm; *inset* 0.02 mm (**A–C** ×150; *inset* ×300; SAB method)

Localization of MIP-2-expressing cells

Although weakly positive reactions for MIP-2 were partially seen in the JE of the normal gingival tissue (Fig. 3A), OGE and OSE were negative. Various types of cells seen in gingival connective tissue and periodontal ligament did not express MIP-2.

At 3 h after topical application of LPS, the expression of MIP-2 in JE was enhanced and the number of MIP-2-positive JE cells was increased. The expression of MIP-2 gradually enhanced over time. According to the overexpression of MIP-2 in the JE, the number of PMNs infiltrated in the JE and sub-JE area increased. At 1 and 2 days after LPS application, almost all cells in the JE were intensively positive for MIP-2 (Fig. 3B). In this period, numerous PMNs were seen in widely enlarged intercellular spaces between MIP-2-positive JE cells. These PMNs were also positive for MIP-2. Both the intensity of MIP-2 expression and the number of MIP-2-positive cells decreased at day 3 (Fig. 3C) and returned to normal range by day 7. There was no MIP-2 expression in the gingival connective tissue and periodontal ligament throughout the experimental periods.

Localization of CINC-2α expression cells

Figure 4 illustrates the localization pattern of CINC-2α protein in the dentogingival junction of control and experimental rats. Positive reactions for CINC-2α were seen in a small number of JE cells in control rats. Especially strong positivity was seen in the coronal half of the JE

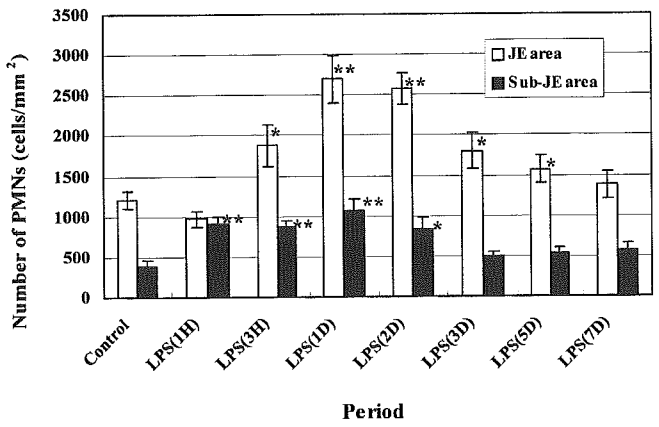

Fig. 5 Number of PMNs in the JE area and sub-JE area (cells/mm^2) after topical application of LPS. n=20 for each group. *Asterisks* indicate a significant difference compared with the value in control group. * P<0.05; ** P<0.01

(Fig. 4A). Some basal cells in the oral sulcular epithelium were positive for CINC-2. LPS application enhanced CINC-2 expression in gingival tissue. CINC-2 expression in the JE was enhanced and many epithelial cells were positive for CINC-2 at 1 day after LPS application. In addition to intensely positive stained cells of the JE in its coronal half, several cells in its apical part and PMNs were weakly positive for CINC-2 (Fig. 4B). At 3 days after LPS application, CINC-2 expression was remarkably reduced (Fig. 4C).

In addition, the epithelial remnants of Malassez show the staining of CINC-2 (Fig. 4A *inset*). Positive staining in the epithelial remnants of Malassez was constantly observed through the experimental period.

Histometric findings

The temporal changes in the number of PMNs in sub-JE and JE areas are demonstrated in Fig. 5. In the untreated control group, the mean number of PMNs in sub-JE and JE areas was 394.5±58.9 and 1,209.3±106.2 cells/mm^2, respectively. In the sub-JE area, PMNs increase from 1 h to 2 days after LPS treatment (P<0.01 at 1 and 3 h and 1 day; P<0.05 at 2 days) and then decreased. However, in the JE area, the mean number of PMNs increased gradually and reached a maximum (2,692.4±287.4 cells/mm^2) at 1 day and then gradually decreased. Significant differences were detected from 3 h to 5 days (P<0.01 at 1 and 2 days; P<0.05 at 3 h and 3 and 5 days).

Discussion

The CXC chemokines are powerful mediators of PMN recruitment. A representative member of the CXC chemokines is IL-8, which is a major chemoattractant for PMNs in humans (Oppenheim et al. 1991; Wirthlin and Hussain 1992). In rats, no homologue to IL-8 has been identified. So far, four CXC chemokines, including CINC (or CINC-1), CINC-2α, CINC-2β, and MIP-2 (or CINC-3), have been identified in rats (Nakagawa et al. 1994; Driscoll et al. 1995; Shibata et al. 1996). They are structurally related to one another and share many functions. It has been demonstrated that they have an ability to attract PMNs and have effects on other PMN functions, including adhesion molecule expression, intracellular calcium influx, and phagocytosis (Nakagawa et al. 1994; Shibata et al. 1995). It was also reported that CINC-2α and MIP-2 were the major chemoattractants in conditioned medium of the granulation tissue. The chemotactic potency of CINC-2α and MIP-2 is higher than that of CINC-1 at a concentration of 1–10 nM (Shibata et al. 1996). Takano and Nakagawa (2001) also reported that CINC-2 and MIP-2 (CINC-3) play an important role in PMN recruitment in the rat air pouch/LPS-induced inflammation. In the present study, therefore, we immunohistochemically examined the expression of MIP-2 and CINC-2 (CINC-2α and CINC-2β) in rat periodontal tissues after LPS challenge.

In untreated control animals, we observed that JE cells, especially in the coronal half of the JE, constitutively expressed MIP-2 and CINC-2. In addition, a minimum number of PMNs were also constantly seen in JE and sub-JE areas. These CXC chemokines produced from JE cells may be responsible for PMN recruitment in JE and sub-JE areas under physiological conditions. Gamonal et al. (2000) examined the levels of IL-1, IL-8, IL-10, and RANTES in gingival crevicular fluid from clinically healthy gingival site. They demonstrated that IL-8 was the only cytokine detected in gingival crevicular fluid from healthy sites and that their concentrations were relatively lower than those in gingival crevicular fluid from inflamed sites. Tonetti et al. (1994, 1995) revealed that focally distributed IL-8 mRNA positive cells were constitutively detected in the JE and suggested that IL-8 expression in the JE may be important for the maintenance of a host–parasite equilibrium in the gingival sulcus.

LPS application caused transient overexpression of MIP-2 and CINC-2 in JE cells with a peak at 1 and 2 days. Corresponding with this peak, a significant increase of PMNs in JE and sub-JE areas was seen. Therefore, an excessive production of MIP-2 and CINC-2α from JE cells may be responsible for selective PMN recruitment from blood vessels and migration into the gingival sulcus through the JE. A similar pattern of IL-8 production accompanied by PMN infiltration has been reported in a variety of mucosal infections (Svanborg et al. 1999; Suzuki et al. 2000). For example, colonic epithelial cells continuously exposed to pathogenic bacteria produced TNF-α in response to bacterial invasion, and TNF-α was able to activate the inflammatory response in the intestinal mucosa by secondarily upregulated IL-8 and MCP-1 production from the epithelial cells (Suzuki et al. 2000).

Several in vitro and in vivo studies showed that gingival epithelial cells are a major source of various cytokines and chemokines in response to periodontal pa-